MODELING AND THERMO-ECONOMIC ANALYSIS OF A PHOTOVOLTAIC-BATTERY-GRID HYBRID ENERGY SYSTEM: A CASE STUDY IN YENIKALE GEOTHERMAL HEAT CENTER

A Thesis Submitted to
the Graduate School of Engineering and Sciences of
İzmir Institute of Technology
in Partial Fulfillment of the Requirements for the Degree of

MASTER OF SCIENCE

in Energy Engineering

by
Gökçe USLU

July 2023
İZMİR

We approve the thesis of **Gökçe USLU**

Examining Committee Members:

Prof. Dr. Gülden Gökçen AKKURT

Department of Energy Systems Engineering, İzmir Institute of Technology

Prof. Dr. Mousa MOHAMMADPOURFARD

Department of Energy Systems Engineering, İzmir Institute of Technology

Doç. Dr. Koray ÜLGEN

Energy Department of Güneş Institute

17 July 2023

Prof. Dr. Gülden Gökçen AKKURT

Supervisor, Department of Energy Systems Engineering
İzmir Institute of Technology

Dr. Hüseyin Utku HELVACI

Co-Supervisor Department of Mechanical Engineering
Doğuş University

Prof. Dr. Gülden Gökçen AKKURT
Head of the Department of Energy Engineering

Prof. Dr. Mehtap EANES
Dean of the Graduate School of Engineering and Sciences

ACKNOWLEDGEMENTS

I would like to express my heartfelt appreciation to Prof. Dr. Gülden GÖKÇEN AKKURT for her valuable guidance and support throughout my research. I also want to thank my co-advisor Hüseyin Utku HELVACI for his assistance and support during my research journey. Additionally, I want to extend my deep gratitude to Prof. Dr. Mousa MOHAMMADPOURFARD and Zahra HAJIMOHAMMADI for their significant contributions to my work.

I would like to express my gratitude to TUBITAK-NCBR Project (No: 118Y490-POLTUR3/Geo4Food/4/2019) for providing PV measurement data.

In my early career in the business world, I am indebted to Şahin BAYRAM, the founder of PEM Enerji, and Ceyhun BİLSAN, the General Manager of DPM Enerji, for enlightening me with their valuable industry insights. I am grateful to them for sharing their knowledge and expertise, which has greatly contributed to my professional growth.

I would like to express my gratitude to Göksel TOPAL for his motivation during my thesis process.

Finally, I would like to extend my biggest thanks to my father, Ilhami USLU, my mother, Gülsüm USLU, and my brother, Halil USLU, for their unwavering trust and support.

ABSTRACT

MODELING AND THERMO-ECONOMIC ANALYSIS OF A PHOTOVOLTAIC-BATTERY-GRID HYBRID ENERGY SYSTEM: A CASE STUDY IN YENIKALE GEOTHERMAL HEAT CENTER

Water is vital for agriculture accounting 50-70% of the total global use of fresh water for irrigation. Geothermal water as a renewable energy source is used to generate electricity, heat and cool. The remaining water can be desalinated to be used for agricultural irrigation. Energy demand of desalination systems is high and mostly rely on fossil fuels increasing cost and greenhouse gas emissions. Thus, renewable energy use in desalination process is increasing. Based on a research project, a pilot desalination system is installed in Yenikale Heat Center of Balcova-Narlidere Geothermal District Heating System to desalinate geothermal water and use for agricultural irrigation. The desalination system is powered by a solar PV system which meets energy need entirely in summer but only 30-50% in winter. The remaining energy need is supplied from the grid. The aim of this study is to maximize the utilization of solar energy for the desalination process while minimizing reliance on the grid. To achieve this objective, three different scenarios are analyzed based on three different solar radiation values of 2021 integrating a battery system. For each scenario; first, battery capacities and the number of PV panels are determined. Then, energy, exergy and exergo-economic analysis are conducted. The parameters calculated in economic analysis are net present value, payback period and cost of energy production. One of the main results obtained is the unit energy cost for solar driven desalination system 0.28 $/kWh which is in a good agreement with the literature (0.214-0.23 $/kWh).

Keywords: Solar Photovoltaics, Battery, Exergo-economic, TRNSYS, Reverse Osmosis

ÖZET

FOTOVOLTAİK-BATARYA- ŞEBEKE HİBRİT ENERJİ SİSTEMİNİN MODELLENMESİ VE TERMO-EKONOMİK ANALİZİ: YENİKALE JEOTERMAL ISI MERKEZİNDE BİR VAKA ÇALIŞMASI

Su, sulama için toplam küresel tatlı su kullanımının % 50-70'ini oluşturan tarım için hayati öneme sahiptir. Yenilenebilir enerji kaynağı olarak jeotermal su, elektrik üretimi, ısı ve soğutma için kullanılır. Kalan su, tarımsal sulama için kullanılmak üzere arıtılabilir. Arıtma sistemlerinin enerji tüketimi yüksektir ve çoğunlukla fosil yakıtların maliyeti ve sera gazı emisyonlarını artırmasına dayanır. Böylece arıtma sürecinde yenilenebilir enerji kullanımı artmaktadır. Balçova-Narlıdere Jeotermal bölge ısıtma Sisteminin Yenikale ısı Merkezinde jeotermal suyu arıtmak ve tarımsal sulamada kullanmak üzere bir araştırma projesi kapsamında pilot arıtma sistemi kurulmuştur. Arıtma sistemi, yaz aylarında enerji ihtiyacını tamamıyla karşılayan, ancak kışın yalnızca %30-50'sini karşılayan PV sistemi ile çalışır. Kalan enerji ihtiyacı şebekeden karşılanır. Bu çalışmanın amacı, şebekeye olan bağımlılığı en aza indirirken, arıtma işlemi için güneş enerjisinin kullanımını en üst düzeye çıkarmaktır. Bu amaca ulaşmak için 2021 yılında Narlıdere'de bir akü sistemi entegre edilerek üç farklı güneş radyasyonu değerine göre üç farklı senaryo analiz edilmiştir. Her senaryo için; öncelikle akü kapasiteleri ve PV panel sayısı belirlenir. Daha sonra enerji, ekserji ve eksergo-ekonomik analizler yapılır. Ekonomik analizde hesaplanan parametreler net bugünkü değer, geri ödeme süresi ve enerji üretim maliyetidir. Elde edilen ana sonuçlardan biri, literatürle iyi bir uyum içinde olan (0,21-0,23 $/kWh) 0,28 $/kWh olan güneş enerjili arıtma sistemi için vebirim enerji maliyetidir.

Anahtar kelimeler: Solar Fotovoltaik, Batarya, Exergo-ekonomi, TRNSYS, Ters Osmoz

TABLE OF CONTENTS

LIST OF FIGURES

Figure **Page**

LIST OF TABLES

Table **Page**

LIST OF SYMBOLS

A	Area	m^2
En	Energy	W
Ex	Exergy	W
E_{batt}	Battery capacity	W
E_{tot}	Overall annual energy production	kWh/year
E_{LD}	Daily energy requirement	Wh/day
E_{SD}	Daily amount of radiation per unit area	Wh/m^2day
I	Current	A
n	Number of autonomy days	-
P	Power	W
S_T	Solar irradiance	W/ m^2
T	Temperature	K
U	Overall heat transfer coefficient	W/m^2K
V	Voltage	V
υ	Velocity	m/s

Greek Letters

ŋ	Efficiency

Subscripts

amb	Ambient
b	Battery
in	Inside, internal
m	PV module
MP	Optimum
OC	Open circuit
out	Outside, external
PCU	Inverter
sun	Sun
s	Total system
solir	Solar radiation
w	Wind

CHAPTER 1

INTRODUCTION

Water is of vital importance for the survival of living things on earth. The increase in the world population, industrialization, pollution caused by the energy production from fossil fuels, climate change and the change in people's consumption habits increase the demand for fresh water. Because out of all the water on earth, 97% is seawater while only 3% is freshwater. In particular, it puts serious pressure on the supply of fresh water. The pressure on the supply of fresh water can be experienced in rural areas far from water sources and in urban areas that expand unevenly. In addition to industrialization, climate change and human factors, the deterioration of water quality and diminishing financial resources also pose a threat to freshwater that will lead to water scarcity. It is predicted that future water scarcity will slow down economic development, negatively affect human health and cause environmental problems.

UNESCO reported that on behalf of UN-Water, 46% of the world's population, approximately 3.6 billion people, do not have access to freshwater sources. A quarter of the world's population has access to water resources but lacks adequate desalination facilities to obtain fresh water. By 2030, up to 40% of the world's population will be affected by water scarcity.

According to another report published by World Resources Institute most of the countries will be affected by water scarcity by the year 2040. As can be seen Figure 1, in fact, currently approximately one-fifth of the world’s population is already experiencing water scarcity.

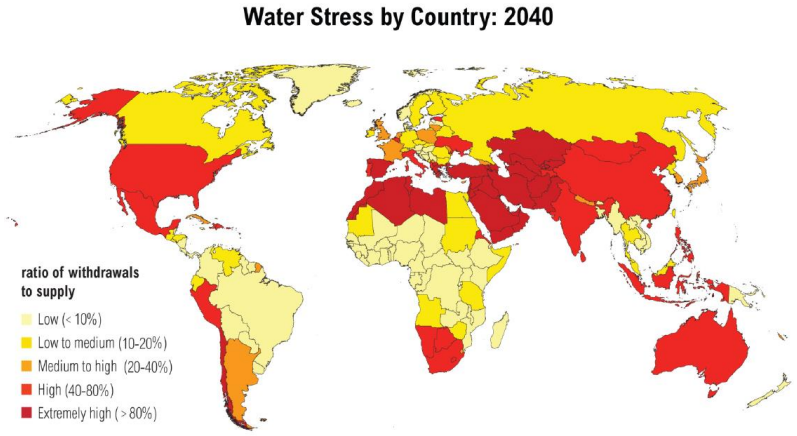

Figure 1. Water scarcity by country: 2040 (WRI 2015)

When considering Türkiye as an example among countries; although Türkiye is surrounded by seas on all three sides, unfortunately not a water-rich country. It is the countries that suffer from water shortage with approximately 1500 m^3/y of water per capita, which is determined as a minimum by the United Nations (Bundschuh et al. 2021). Considering that the population of Türkiye will reach 100 million by 2030, it is estimated that the amount of water per capita will decrease by 1,120 m^3/y. Türkiye will become poor in water with population growth, industrialization and growing cities. The fresh water need of Türkiye is provided from 25 major main basins as shown in Figure 2. Approximately 35% of Türkiye's fresh water requirements are fulfilled by the Meriç, Aras, Çoruh, Fırat-Dicle, and Asi river basins (Hakyemez 2019).

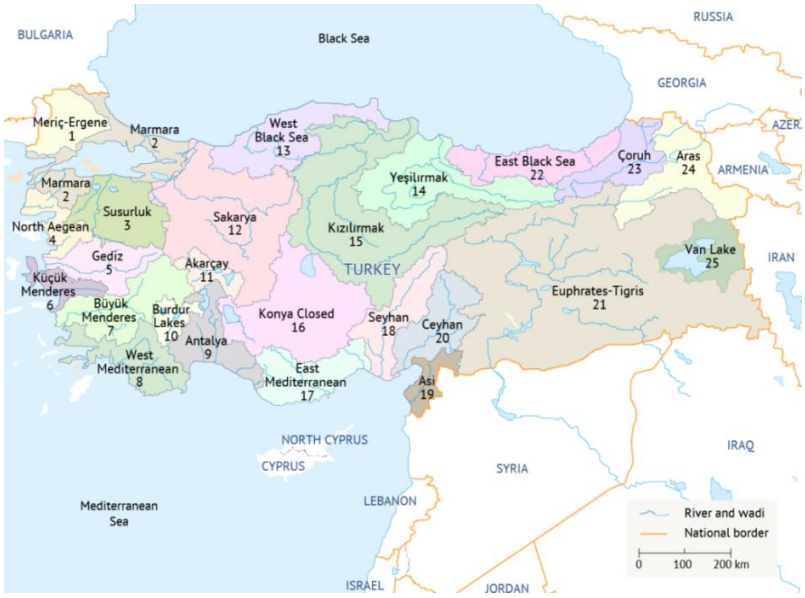

Figure 2. Fresh water resources of Türkiye (Fanack Water 2022)

According to Figure 2, out of the water produced by the 25 major river basins mentioned, 23% is utilized for industrial (10%) and domestic purposes (13%), while the remaining 77% is utilized for agricultural purposes. If we evaluate the water usage ratios in Türkiye, specifically for İzmir where the project is located, according to the data provided by İzmir Metropolitan Municipality, İzmir's annual water consumption is 257,905,385.75 m^3 (IMM 2023). As shown in Table 1, 25.70% is used for drinking water, 21.80% is used in industry, and 52.50% is used for agricultural irrigation. When interpreting these values, it can be concluded that the rate of 52.50%, which corresponds to more than half of the total water consumption, is used in agricultural practices. Additionally, 57.05% of the water demand in Izmir is met by dams, while 42.95% is met from underground water sources.

Table 1. Izmir sectoral water consumption (Gol 2021)

Usage Area	**Amount of Usage (m^3)**	**Rate (%)**
Drinking water	66,281.684.14	25.70
Industry	56,223,374.09	21.80
Agricultural	135,400,327.52	52.50

Considering factors such as unconsciousness in water use, water pollution, climate change, deterioration of natural water reserves and global warming, there are serious threats to existing water resources in Türkiye. In addition, uncontrolled wastewater discharges, use of chemical pesticides in agriculture, harmful particles from flue gases pose chemical and ecological threats to water sources (Uyduranoğlu Öktem 2015).

As mentioned above, the global and Türkiye water scarcity, along with the need for freshwater usage in agricultural, domestic and industrial sectors has highlighted the importance of freshwater production through desalination methods using seawater and brackish water sources. Desalination, which involves filtration processes that remove salts and other minerals from salty and brackish water, is one of the solutions to the problem of water scarcity that meets the demand for fresh water. In desalination processes, the provision of heat or electrical energy is required for fresh water production.

Desalination technologies are divided into thermal and membrane processes. Thermal desalination technologies are divided into vapor compression distillation (VCD), multi-effect distillation (MED) and multi-stage flash distillation (MSF). Membrane desalination technologies are reverse osmosis (RO), electrodialysis (ED) and forward

osmosis (FO). The MSF, RO and MED technologies are the most widely used desalination technologies. Membrane desalination systems require high pressure to separate permeate from seawater or brackish water. This process consumed electricity. In thermal desalination, heat is used to evaporate the permeate water. Therefore, thermal desalination systems are more expensive in terms of cost because they require both electricity and heat. As stated, the reverse osmosis desalination system is the focus of the thesis. Therefore, the flow diagram of the reverse osmosis desalination system is also presented separately. Figure 3 illustrates the flow diagram of a RO water desalination system. A standard reverse osmosis (RO) system is comprised of four main components: pre-desalination system, high-pressure pump, membrane module, and post-desalination system. First, pre-desalination is performed to remove large particles, dust, and sand from the water. The pre-desalinated water is then pressurized using a high-pressure pump to pass through reverse osmosis membranes. Reverse osmosis membranes consist of porous layers that allow the passage of water molecules while blocking the passage of other particles. The water that passes through the reverse osmosis membrane is referred to as purified water. Contaminants and other particles that cannot pass through the membrane are concentrated and removed from the system. Finally, post-desalination is carried out to further enhance the quality of the water obtained after reverse osmosis, making it even cleaner and suitable for drinking.

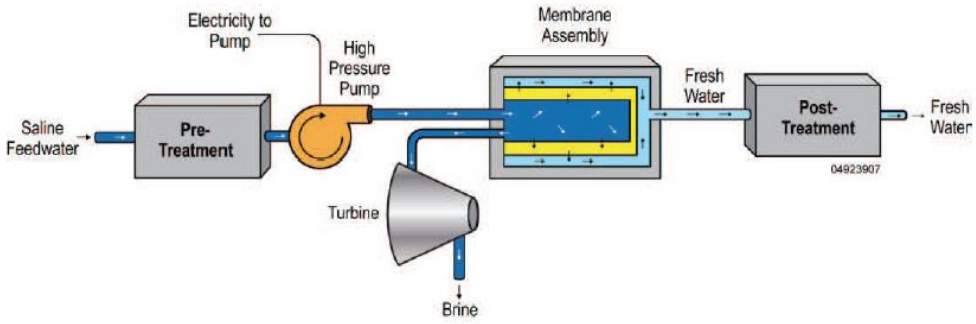

Figure 3. Reverse osmosis process diagram (Al-Karaghouli and Kazmerski 2011)

The cost of desalination technologies is determined by the salt content of the feed water, quality of the product water, energy cost and the system dimensions(Alatiqi, Ettouney, and El-Dessouky 1999). The water production costs of different desalination systems are shown in Figure 4. Figure 4 presents the thermal desalination systems, including Multi-Effect Distillation (MED) and Multi-Stage Flash (MSF), as well as the

membrane desalination system, Electrodialysis (ED). The aim of the figure is to illustrate the cost in $ per cubic meter (m^3) of water production for different desalination systems. In terms of cost, the water production for the MED desalination system ranges from the highest value of 1.6 $/$m^3$ to the lowest value of 0.6 $/$m^3$. The MED system exhibits the highest cost among the presented desalination systems. On the other hand, the lowest costs per m^3 are observed in the ED desalination system, ranging from the highest value of 0.75 $/$m^3$ to the lowest value of 0.26 $/$m^3$. Also, Figure 5 displays the costs of reverse osmosis desalination systems in different sizes. In reverse osmosis desalination systems, the maximum cost of water decreases from 2.46 $/$m^3$ at the large scale to 1.25 $/$m^3$ at the small scale. Similarly, the minimum cost of water decreases from 0.36 $/$m^3$ to 0.14 $/$m^3$ across the same scale range.

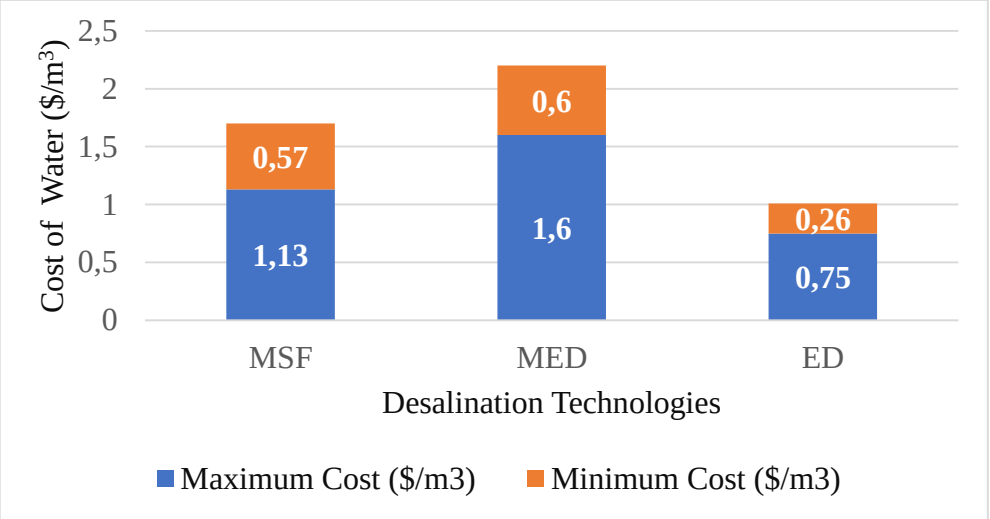

Figure 4. Cost of water using MSF, MED, ED (Eke et al. 2020)

.

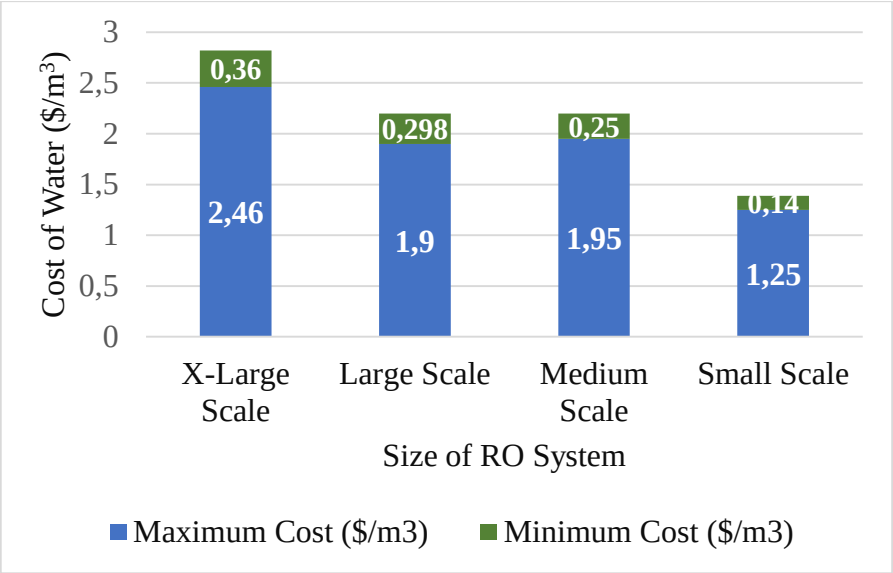

Figure 5. Cost of water using RO (Eke et al. 2020)

When considering energy consumption, it still varies depending on the choice of the desalination system. Desalination system consume 8-20 times more energy than conventional desalination systems such as coagulation and flocculation, sedimentation filtration disinfection, pH adjustment and fluoridation (Voutchkov 2018). The energy consumption according to the desalinated waters are provided in Table 2.

Table 2. Energy consumption required for 1 m^3 of fresh water (Voutchkov 2018)

Water Source	**Energy Consumption (kWh/m^3)**
Traditional desalination of surface water	0.20-0.40
Ground water	0.48
Wastewater desalination	0.62-0.87
Wastewater reuse	1.00-2.50
Brackish water desalination	1.00-1.50
Seawater desalination	2.58-8.50

Table 3 illustrates the energy consumption of different desalination systems. As seen, membrane technologies require both electrical and thermal energy consumption. Specifically, in thermal desalination technologies like MSF and MED the energy consumption ranges from 13.5-25.5 kWh/m^3 and 6.5-11 kWh/m^3 respectively. In RO desalination systems, an energy consumption of 3-7 kWh/m^3 is observed.

Table 3. Energy consumption of different desalination technologies (Alkaisi, Mossad, and Sharifian-Barforoush 2017)

Desalination Technologies	**Water Type**	**Electricity Consumption (kWh/m^3)**	**Thermal Energy Consumption (kJ/kg)**	**Electricity Consumption Equal to Thermal Energy (kWh/m^3)**	**Total Energy Consumption (kWh/m^3)**
MSF	Seawater, brackish water	4-6	190-390	9.5-19.5	13.5-25.5
MED	Seawater, brackish water	1.5-2.5	230-390	5-8.5	6.5-11
MVC	Seawater, brackish water	7-12	-	-	7-12
RO	Seawater, brackish water	3-7	0	0	3-7
ED	Brackish water	2.6-5.5	0	0	2.6-5.5

Meeting the energy requirements of desalination technologies with renewable energy sources instead of fossil fuels is not environmentally but also cost-effective (Zhang et al. 2023) Selection of renewable energy source suitable for desalination technologies depends on many factors such as the size of the facility, the salinity of the feed water, the distance to the electricity grid, its technical infrastructure and renewable energy potential(Al-Karaghouli and Kazmerski 2011). Türkiye is particularly advantageous compared to many other countries in terms of renewable energy sources such as solar, wind, and geothermal, which will facilitate the utilization of renewable energy in meeting the energy demand of desalination technologies (IEA 2021). The hybrid utilization of renewable energy sources such as solar/wind (Gomaa et al. 2023) or solar/geothermal (Stefano et al. 2021) in desalination systems will further reduce energy and water production costs.

Table 4 shows the renewable energy sources used in different desalination technologies. As shown in Table 4, solar and wind energy are the most widely used renewable energy sources in desalination systems. Solar and wind energy can be used both separately and in hybrid form in desalination systems.

Table 4. Renewable energy with desalination technologies (Al-Karaghouli and Kazmerski 2011)

Source of Renewable Energy	Type of Feed Water	Type of Desalination Technologies				
		VC	ED	RO	MSF	MED
Photovoltaic (PV)	Seawater			X		
	Blackrish water		X	X		
Solar thermal	Seawater				X	X
Geothermal	Seawater					X
Wind	Seawater	X		X		
	Blackrish water			X		

Table 5 shows the desalination capacity and cost of water of wind and solar-assisted desalination systems. The table illustrates that the cost of water production in solar energy-based desalination systems is lower than in wind energy-based systems. Factors such as capacity, radiation levels in the region, salinity of the water, and regional electricity prices are important parameters in determining the cost of water in PV assisted systems. Currently, PV, battery, and grid-supported desalination technologies are more common compared to wind-supported technologies because of the decreased cost of PV panels and batteries over the years.

Table 5. Capacities of different desalination systems and freshwater production costs

Desalination System		Desalination Capacity (m^3/d)	Cost of Water ($/m^3$)
PV-RO(Ajiwiguna et al. 2021)		1000	1.74-2.59
PV-RO (Ajiwiguna et al. 2021)		50000-190000	0.89-1.80
PV-RO (Ahmad and Schmid 2002)	PV	254000	2.27
	PV-battery	254000	1.58
	PV-grid	254000	0.89
PV-RO (Ghaithan, Mohammed, and Hadidi 2022)	PV-grid	60000	0.88
	PV-battery	60000	2.14
	PV-grid-battery	60000	0.95
PV-RO-battery (Ajiwiguna et al. 2022)		1000	10.80
Wind-RO(Abdelkareem et al. 2018)		50-2000	6,60-900
PV-RO (Abdelkareem et al. 2018)		<100	6.50-9.10
PV-SWRO (Abdelkareem et al. 2018)		<100	11.70-15.60
PV-SWRO (Abdelkareem et al. 2018)		250	45019
Wind-RO (Abdelkareem et al. 2018)		50-2000	2-5.20

Türkiye has an important solar energy potential due to its geographical location. According to the Solar Atlas of Türkiye, the average daily and annual sunshine durations are 7.5 h and 2741 h, respectively. The average annual solar radiation value is calculated as 1527.46 kWh/m^2. Figure 6 shows the monthly average radiation values of Türkiye (MENR 2022).

According to Figure 6, the highest radiation value is observed in June and July, which is 6.5 kWh/m^2. The lowest monthly radiation values are observed in December and January, which are 1.59 kWh/m^2 and 1.79 kWh/m^2, respectively. For the other months, an increase in radiation values can be observed from March to May, while radiation values start decreasing from August onwards.

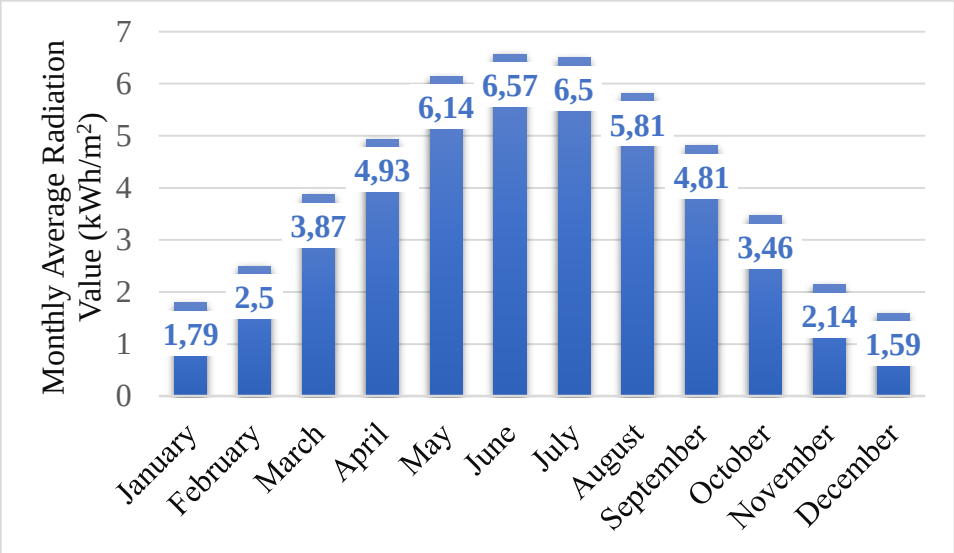

Figure 6. Monthly average radiation values of Türkiye (MENR 2022)

As shown in Figure 7, installed solar power capacity of Türkiye has been increasing over the years and it is expected that regarding with Türkiye's renewable energy policies and investment incentives will increase the installed power in solar energy in the coming years (IEA 2021).

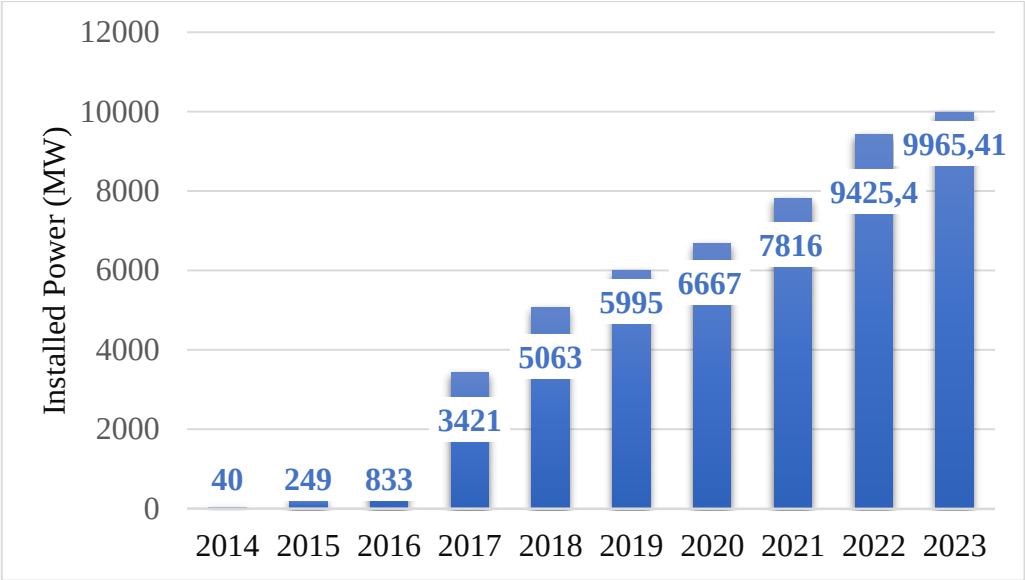

Figure 7. Installed solar power plant capacity of Türkiye (TEIAS 2023a)

As of May 2023, Türkiye capacity in electricity generation reached to 9965.4 MW with a share of 9.5% in total installed power capacity (TEIAS 2023a, 2023b).

Solar energy can power desalination plants as heat and/or electrical energy generated from by PVs.

1.1 Motivation

As mentioned before, due to reasons such as global warming, irresponsible water management, and rapidly increasing population growth, access to clean water is becoming increasingly challenging. When considering the global water resources, it corresponds to a rate of 23%. Therefore, it is becoming crucial to turn towards alternative methods for obtaining clean water. The most preferred method among these techniques is water purification technology. An example of this is the project carried out in Yenikale, Izmir, where geothermal waters from the Yenikale geothermal heat center are desalinated and used for agricultural irrigation. The desalination is done using a solar-assisted reverse osmosis system. In this solar-supported desalination system, the fulfillment of the desalination load varies depending on the seasons. Throughout the year, during the summer months, there is an excess of PV production compared to the desalination load, while in the winter months, it falls short, and grid electricity is used to meet the demand. The goal is to maximize the utilization of solar energy, aiming to cover 100% of the desalination load from solar power, thereby minimizing reliance on the grid.

In this regard, new components such as batteries have been added to the system to enable the storage of excess energy generated during periods of high electricity production from the solar panels and utilize it on days when there is no production. It also aims to reduce electricity costs by using stored energy during evening peak hours, when electricity prices are high, according to electricity rates, and supporting the grid during morning hours.

The novelty of this study is to support the utilization of desalinated geothermal wastewater for agricultural irrigation, thereby enhancing crop yield. Typically, desalination processes involve the use of seawater and brackish water rather than geothermal waters. A pilot desalination system has been set up within the Yenikale Heat Center of the Balcova-Narlidere Geothermal District Heating System as part of a research project. This system aims to desalinate geothermal water, removing its salinity, in order to make it suitable for agricultural irrigation purposes. Geothermal waters, which are commonly used for electricity generation, heating, tourism, etc., will be desalinated to remove harmful substances before being supplied to plants. Moreover, the energy required for this desalination process will be provided by renewable sources.

CHAPTER 2

LITERATURE SURVEY

The introduction mentioned the effects of population growth, increasing industrialization, and climate changes on water and energy. In particular, emphasized that countries may face serious difficulties in accessing fresh water sources in the future. In order to prevent scarcity that may occur in freshwater resources, it is necessary to use existing sources consciously and to apply desalination technologies as an alternative method.

2.1. History of Desalination Technologies

The first studies on Desalination Technologies were made during the Second World War to meet the fresh water needs of remote regions. Desalination Technologies have been used commercially since 1960 and the first method used was thermal desalination. MSF systems, which are thermal desalination systems, began to be used more widely in the 1960s and the first examples were installed in the Persian Gulf (Reddy and Ghaffour 2007). Membrane desalination technologies entered the market commercially in the 1960s and were first used for brackish water desalination. In the 1980s, both thermal technologies and membrane technologies began to be used commercially in the world (Cooley, Gleick, and Wolff 2006). Countries using desalination technologies are shown in Figure 8.

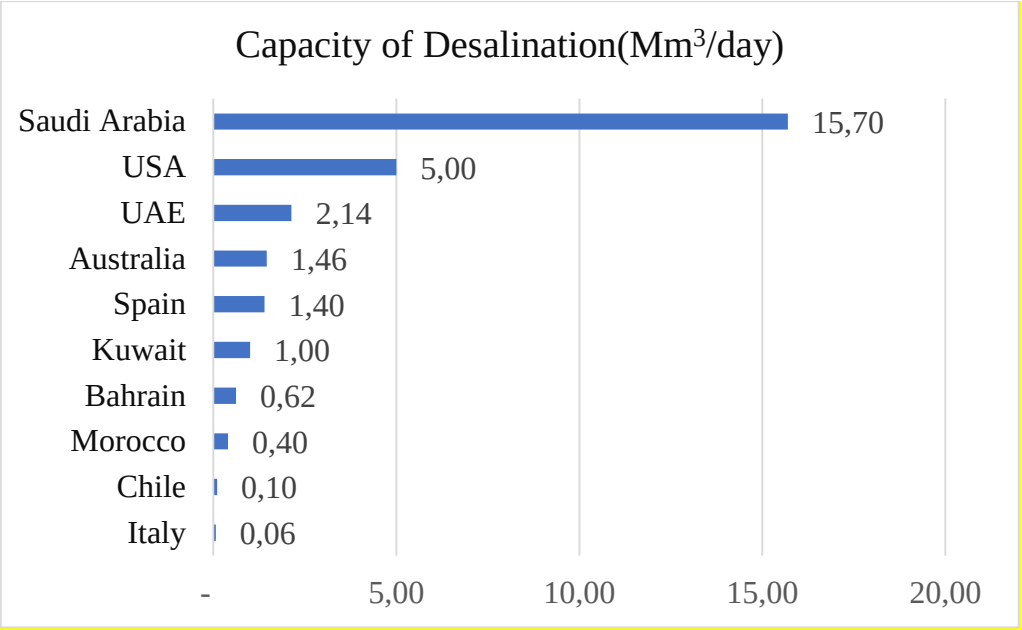

Figure 8. Countries using desalination technology (Kumar et al. 2022)

2.2. Desalination Applications with Renewable Energy

Desalination technologies can be used in areas where there is no grid connection or far from the grid, by integrating with renewable energy sources according to the renewable energy use potential of the region. The use of desalination systems with renewable energy will be sustainable, environmentally friendly, and economical in obtaining fresh water. Especially as the production costs of renewable energy sources decrease, these systems will become more economically attractive. Today, almost 1.2% of Desalination technologies are powered by renewable energy sources (Sarathe et al. 2022). Renewable resources such as solar energy, wind energy, and geothermal energy such as PV and thermal are used to meet the energy demands of desalination technologies. In addition, in desalination technologies using renewable energy, different combinations of storage technologies can be used to store energy in cases where excess energy is produced (IRENA 2012). In the technical feasibility of desalination technologies using renewable energy, parameters such as location, inlet of feed water, and quality of fresh water to be obtained, available renewable energy capacity, and size are taken into consideration. In addition, the operation and maintenance requirements of the facility, the transfer of feed water and the demand for pre-desalination should also be considered.

2.2.1. Desalination with Solar Energy

Solar energy, a sustainable and renewable energy source, possesses significant potential on our planet. The Earth receives solar radiation at levels as high as 120 petawatts (PW). According to studies, it is predicted that the energy provided by the sun in one day will meet the world's energy needs for 20 years (Chu and Meisen 2011). Integration of solar energy with desalination technologies will be one of the most promising technologies in the future due to their environmentally friendly nature. Solar powered desalination technologies are divided into two as thermal and photovoltaic systems.

2.2.1.1. Desalination with Solar Thermal

These technologies are systems that utilize solar energy to obtain thermal or heat energy. These systems consist of flat or parabolic solar collectors and mirrors or lenses to maximize the utilization of solar rays. Collectors absorb solar radiation and transfer the absorbed solar energy to a fluid flowing within them. The absorbed heat can be subsequently utilized for heating systems or to generate electricity by operating heat engines (Pouyfaucon and García-Rodríguez 2018). Various collectors are used in thermal systems depending on their operating temperatures. Concentrated Solar Power (CSP) systems, as shown in Figure 9, are used for high temperatures, while flat plate collector systems are used for lower temperatures. There are various types of CSP, including parabolic trough collectors, parabolic dish collectors, heliostat field collectors, and Fresnel collectors (Malviya, Agrawal, and Baredar 2021). Desalination systems utilizing solar thermal technologies can be integrated with membrane units such as reverse osmosis (RO) and thermal desalination units such as multi-stage flash (MSF) and multi-effect distillation (MED). CSP facilities are also utilized in medium to large-scale seawater desalination plants.

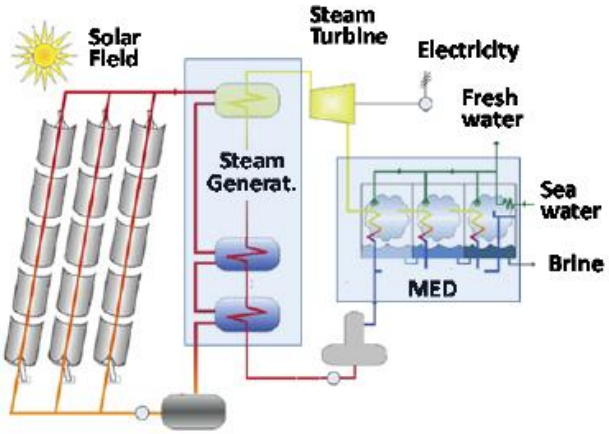

Figure 9. CSP power station and MED desalination system (Zachary and Layman 2010)

Koschikowski et al. (Koschikowski, Wieghaus, and Rommel 2003) have designed a small-scale system to meet the demand for potable water in rural and semi-arid areas by desalinating brackish water from wells or saltwater from the sea. This system is based on a separation technique called membrane distillation. The capacity of the membrane distillation system is planned to be in the range of 0.2 to 20 m^3/d, and the energy required will be supplied by solar power. The heat from the sun is collected through a corrosion-resistant thermal collector, standard flat plate, and vacuum tube collectors, and performance analyses through simulations have been conducted for three different regions. The simulations have shown that Eilat achieves a maximum drinking water production of 28 l/d during the summer months, while the minimum water production of 11 l/d is obtained in December. It has been observed that adding heat collector panels to the membrane distillation system improves its efficiency, and it has been determined that with an area of less than 6 m^2, the maximum water production capacity can reach levels of 150 l/d. Furthermore, ongoing investigations at Fraunhofer ISE focus on developing new membrane distillation modules with lower Gain Output Ratio (GOR) and pressure values.

Karellas et al. (Karellas, Terzis, and Manolakos 2011) have designed a desalination system where solar energy collectors support a reverse osmosis system through an Organic Rankine Cycle. The power demand of the Organic Rankine Cycle is met by a hybrid system based on a PV generator. An inverter is used to convert DC to AC power, and a battery array is employed for energy storage. The complete operation of the system is examined, taking into account the pumping loads from the sea and to the

municipal water network. The study aims to address the shortage of potable water and design an autonomous desalination system for situations where there is no electrical grid. The design of this PV and the solar thermal-supported system is conducted using the Homer program. The hybrid desalination system is planned to have a water capacity of 83,000 m^3/y. Based on the analysis, it is concluded that the best scenario for the cost-effectiveness of the project is to subsidize 40% of the investment capital of the facility. Additionally, the cost of clean water production is calculated to be 6.55 €/m^3.

Diego and Karen (Cunha and Pontes 2022) have proposed a thermal desalination technology from brackish water for freshwater production in Brazil's semi-arid region. The main objective of the study is to propose a small-scale desalination system integrated with solar energy for brackish water desalination in Brazil and to evaluate its technical and economic feasibility. What sets this study apart from similar works in the literature is its ability to produce fresh water solely using solar energy. After conducting a detailed cash flow analysis to assess the economic feasibility of the facility, the estimated water production cost for a facility with a capacity of 72 m^3/d is 4.95 \$/m^3. The results of the analysis indicate that the designed system is a cost-effective and sustainable alternative to alleviate freshwater scarcity in the Brazilian region.

2.2.1.2. Desalination with Photovoltaic

Photovoltaic (PV) systems are systems that collect solar energy and produce electrical energy using semiconductor material technology. The power output of PV systems is DC. These systems can operate on or off the grid. While DC current is stored in batteries in off-grid systems, it is necessary to convert DC current to AC current using an inverter in grid-connected systems. The performance of photovoltaic systems depends on the amount of radiation, climatic conditions and factors such as panel material (Vidyanandan 2017). An example of PV-RO desalination technology is shown in Figure 10. As seen in the Figure 10, the electrical power requirement of the pumps during the desalination process is met by PV panels and a battery system is also implemented. This way, any excess energy generated by the PV panels during the day can be stored in the batteries, and the stored surplus energy can be utilized during periods when the panels are not providing electricity.

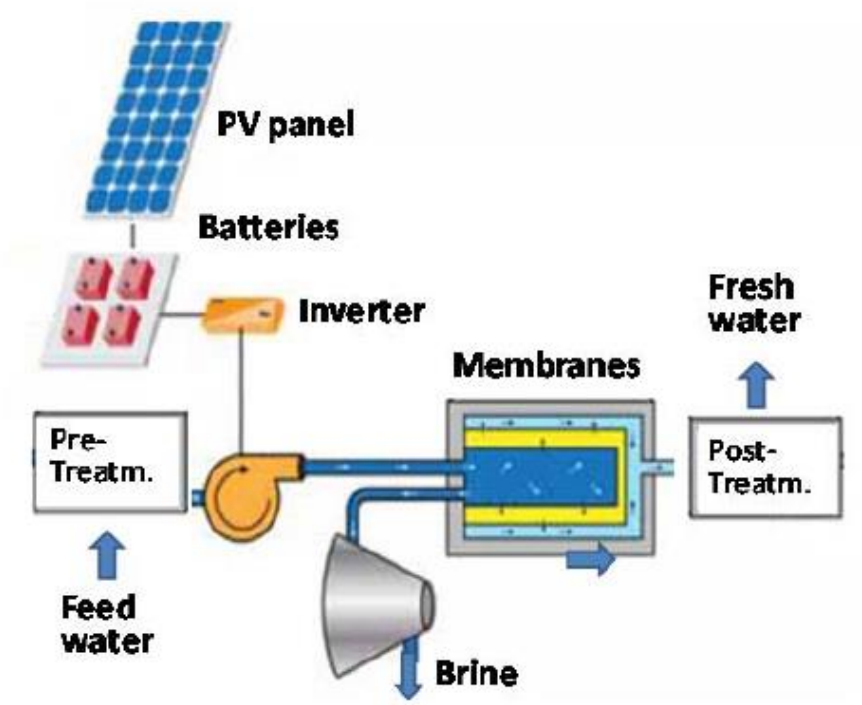

Figure 10. PV – RO integrated desalination system (Al-Karaghouli and Kazmerski 2011)

In the study conducted by Ahmad and Schmid (Ahmad and Schmid 2002) the design of a solar photovoltaic (PV)-supported reverse osmosis desalination plant for Egypt was examined, and a feasibility analysis was conducted. The design involved the integration of a PV system with an inverter and batteries. The energy consumption of the system was determined to be 4 kWh/day. Within the scope of the feasibility analysis, the water production cost in the small-scale PV-supported reverse osmosis system was calculated to be 3.73 $/m^3. Furthermore, the study argues that increasing the size of the system and the daily operating hours would lead to a reduction in freshwater production costs.

Abdel-Ghani et al. (Ahmad and Schmid 2002) conducted a feasibility analysis of three different configurations of a solar-powered reverse osmosis (RO) desalination system with a capacity of 254,000 m^3/day. The first configuration of the PV-RO system was solely PV-powered, the second configuration was PV and battery-powered, and the third was PV and grid-powered. These three configurations were simulated using IMSDesign and PVsyst software. Based on the simulations, the water production costs for each configuration were calculated. The analysis revealed that the water production cost for the PV-powered configuration was 2.279 $/m^3, the PV-battery-powered configuration was 1.585 $/m^3, and the PV-grid-powered configuration was 0.892 $/m^3.

When examining the water production costs, it was determined that the most economical configuration was the PV-grid-supported design. The cost of the PV-battery-powered RO system was calculated as 350.573×10^6 $. It was emphasized that this system would provide water to the future Burj Al Arab city.

A study conducted by Marwan (Marwan M Mahmoud 2003) presented a saltwater desalination project using solar energy-supported reverse osmosis technology based on the climatic conditions of Al Maleh. The performance, techno-economic feasibility, and environmental impacts of the solar-powered reverse osmosis desalination system were examined through simulations. Within the project scope, the required energy for meeting a 10 m^3/day water demand for 5 hours was calculated to be 16 kW. The project utilized 162 solar panels to meet this energy requirement. Additionally, a battery system with a capacity of 27.65 kWh was added to the project to fulfill 1.5 days of load demand. The simulation results demonstrated a linear relationship between water production and solar radiation intensity. Moreover, it was found that the water production cost in the facility was lower compared to desalination systems using diesel generators.

There are studies available that compare only renewable, only nonrenewable or hybrid technologies. For example, Helal et al. (Helal, Al-Malek, and Al-Katheeri 2008) conducted a study on the economic feasibility of an autonomous reverse osmosis (RO) system for remote areas in the United Arab Emirates (UAE). Three alternative configurations of a 20 m^3/day capacity RO system were examined: a diesel generator-based system, a PV-diesel hybrid system, and a battery-less solar panel system. In the diesel generator-based system, the entire energy demand is met by diesel fuel. In the PV-RO system with diesel generator support, diesel fuel is used during nighttime or power outages. In the PV-only system, the energy requirement for 20 m^3/day production is solely supplied by solar panels during daylight hours. Cost calculations were performed for each configuration, and their environmental impacts were evaluated. The economic analysis revealed a water production cost of 7.64 $/$m^3$ for the diesel generator-based system, 7.21 $/$m^3$ for the PV-RO system with diesel generator support, and 7.34 $/$m^3$ for the fully PV-supported system. Furthermore, the specific energy cost was determined to be 2.14 $/$m^3$ for the diesel generator-based system, 1.81 $/$m^3$ for the PV-RO system with diesel generator support, and 1.31 $/$m^3$ for the fully PV-supported system. The study emphasized that in the fully PV-supported system, the cost could be further reduced to

7.34 $/m^3 through activities promoting solar energy utilization, such as reducing capital interest rates, providing tax exemptions, and lowering land costs.

Natasha and Amos (Wright 2014) presented the design criteria for a photovoltaic (PV) supported electrodialysis (ED) system for desalination, intended to meet the water needs of off-grid regions in India. The study compared reverse osmosis (RO) and ED desalination technologies for the Indian context. Considering parameters such as low energy consumption per unit water production, lower capital costs, and higher recovery rates, it was determined that ED is more advantageous than RO systems for the Indian region. The study revealed that ED desalination technologies can be operated directly from a PV array without the need for an inverter.

There are grid-tied system designs available to meet the electricity demand during times when there is no production from the solar panels. Alsheghri et al. (Alsheghri et al. 2015) designed a cost-effective photovoltaic (PV) supported reverse osmosis (RO) desalination system for Masdar Institute of Science and Technology. The system provided grid support against intermittent power generation. Additionally, excess energy generated from solar power was sold back to the grid. A PV design with a capacity of 720 kW and an area of 5038 m^2 was implemented to meet the energy demand of the PV-supported RO technology. The plant's capacity factor was 27.9%, and the annual electricity sold to the grid amounted to 1757.8 MWh. The payback period of the system was calculated as 23.3 years, with a benefit-cost ratio of 0.72. The water production cost of the PV-RO supported system was estimated at 0.825 $/m^3. The study emphasized that solar energy-supported reverse osmosis desalination technologies are efficient alternatives for freshwater production and are expected to become more economically viable in the future.

Karavas et al. (Karavas et al. 2018) investigated the experimental exploration of a small-scale, autonomous reverse osmosis (RO) desalination system based on the concept of a DC microgrid, utilizing hydraulic energy recovery and providing short-term energy storage through hybrid capacitors, operating with photovoltaics (PV). Fuzzy cognitive maps were employed for the system to operate under varying conditions, and an energy management system was developed. The experimental results demonstrated the efficient operation of such a PV-supported RO desalination technology. It was observed that the energy generated from the PV array could be stored and used to produce fresh water in the RO system even on days with low solar radiation. Furthermore, the PV-

RO desalination technology with short-term storage in the energy management system exhibited higher freshwater production on days with variable solar radiation compared to a directly PV-operated RO system without storage or any control mechanism.

In the study by Mostafaeipour et al., (Mostafaeipour et al. 2019) the electrical reliability and costs of off-grid photovoltaic-assisted reverse osmosis desalination systems for 9 counties of Iran's Bushehr province were investigated. In the study, 16 years of solar radiation values and clarity index data were taken as references. Homer and Excel programs were used for the technical-economic feasibility of the systems proposed for 9 districts. By using the fuzzy time function, it has been seen that the reliability of off-grid photovoltaic systems gives better results than the simple method. As a result of the technical and economic analysis, the investment, energy, operation, maintenance, and water production costs of the systems designed for 9 states were calculated. The results of the evaluation of photovoltaic systems by the HOMER software showed that the annual electricity generation for Delvar and Deylam ports was 72,336 and 47,915 kWh, respectively. In addition, drinking water production for Delvar and Deylam ports was calculated as a maximum of 228 m^3/d and a minimum of 148 m^3/d, respectively, while water production costs for Delvar and Deylam could be between 1.96 \$/m^3 and 3.02 \$/m^3. As a result of the study, it was concluded that this system would be more economical for Delvar, which is one of the 9 states, compared to the current 2.5 \$/m^3 water cost.

A new design for desalination system with photovoltaic-assisted reverse osmosis technology suitable for intermittent operation has been presented by Gurmaly and Bilton (Freire-Gormaly and Bilton 2019) to provide more reliable and long-lasting systems. A genetic algorithm based on a simulation model consisting of a physical system model and a cost model was used to evaluate the system cost. 10-year system simulations were made for 1 m^3/day, 5 m^3/day and 10 m^3/day fresh water capacities. The number of PV panels and battery capacities were determined in each simulation. As a result of the simulations, it has been seen that the intermittent operation of the PV-supported RO system is a useful method to reduce the energy storage requirements and reduce the system costs to an achievable range.

Ghafor et al. (Abdul Ghafoor and Munir 2015; A. Ghafoor et al. 2020) conducted a techno-economic analysis of a solar desalination system with 500 l/h capacity, with and without a solar tracker system and solar-powered reverse osmosis technology. The PV-

RO system consists of a 2 kWp solar panel system and a 5 kW hybrid inverter. Performance evaluation of the PV-RO system; produced in terms of energy, membrane efficiency, and economic analysis. As a result of the studies, it has been determined that 40% of the energy for the RO facility is provided by the PV system and 60% from the grid in the winter season, and the business operates between 09:00 and 17:00. It has been determined that 60% of the energy is provided by the PV system and 40% from the grid in the summer season. It has also been observed that the PV energy increases by 15-20% with the PV system with a tracker and by 5-10% with the cooling of the PV panels. The water production cost was calculated as 0.72 $/l and the payback period of the system was calculated as 1.83 years. It was emphasized that the PV-RO system is an economically viable technology and an opportunity for entrepreneurship and income generation for future generations.

Ajiwiguna et al. (Ajiwiguna et al. 2021) developed algorithms for the optimization of a PV-RO desalination technology with a seasonal water storage tank. The capacity of the RO unit is determined according to the operating time between 4 h/d and 10 h/d. In order to compare the systems, two scenarios, fixed and variable freshwater demand, were examined. The optimum inclination angle for the PV modules to be used in the system and the minimum number of modules to meet the annual water demand were determined. Afterward, tank capacities were determined according to daily water production and demand data. To find the optimum sizing of the system components, the water cost analysis of the scenarios was performed. As a result of the analysis, the optimum operating time of the RO unit was determined as 9 h/d for constant water demand and 8h/d for variable water demand. The lowest water costs were calculated as 1.74 $/$m^3$ for fixed water demand and 2.59 $/$m^3$ for variable water demand, respectively. The cost of water (1.74 $/$m^3$) obtained with the optimization algorithm developed within the scope of the study is very competitive compared to other desalination technologies working with renewable energy.

Rahimi et al. (Rahimi et al. 2021) conducted a feasibility analysis for a 2000 m^3/day capacity desalination plant using reverse osmosis technology, considering various PV and grid integration options in a country with low electricity prices. The study examined five different scenarios and assessed the effects of energy recovery equipment, energy storage systems, and membrane properties. A detailed cash flow analysis was conducted for each scenario. The first scenario involved a grid-connected RO system,

while the second scenario utilized PV during the day and grid electricity at night. The third scenario relied on PV during the day (with excess production sold to the grid) and grid electricity during low radiation or nighttime. The fourth scenario focused on selling electricity only, with PV providing the electricity and the grid supplying power to the RO plant. The fifth scenario involved an off-grid system with battery-supported PV. The scenarios were analyzed using Homer software, and the economic models' results were validated with local market data. The capital cost of the reverse osmosis system was estimated at approximately 1270 $/m^3. Based on the analyses, the fourth scenario was identified as the most advantageous, with a water production cost of 1.11 $/m^3 and a payback period of around 6 years. The grid-connected RO scenario had the lowest water production cost at 0.76 $/m^3, while the off-grid scenario had the highest water production cost at 4 $/m^3.

Ajiwiguna et al. (Ajiwiguna et al. 2022) presented a strategy in the design of PV-assisted RO desalination technology that provides battery support to store excess energy and prolong water production operating time. PV-RO with battery and seasonal water storage tank and PV-RO system were examined and water costs were analyzed. Water costs for fixed and variable demand decreased from 10.21 $/m^3 to 2.31 $/m^3, and from 36.96 $/m^3 to 3.06 $/m^3, respectively. At the end of the study, it was emphasized that water production costs will be more competitive in the future, as battery technology is developed and battery prices are expected to decrease by 10-52% in 2025.

In another study conducted by Gaithan et al. (Ghaithan, Mohammed, and Hadidi 2022) technical and economic analyzes of a desalination system with solar-assisted reverse osmosis technology were carried out in four different scenarios by using Deep software. These scenarios are; fully grid-supported, PV-Grid supported, PV-Grid Battery and PV-Battery supported. For these scenarios, the freshwater production capacity was evaluated as 60000 m^3/d. Within the scope of the study, the effect of fuel subsidies on the cost of water desalination and the effect of solar energy on reducing carbon dioxide was investigated. As a result of the analysis, the water production cost of PV-RO technology was found to be highly competitive against conventional reverse osmosis desalination. The inclusion of the battery system in the PV-RO has been found to increase water costs by 8% compared to the PV grid without storage. For the full grid supported scenario, the water production cost is calculated as 1,946 $/m^3, for PV-Grid supported 1,695/m^3, 1,519 $/m^3 for PV Grid-Battery, and 2,141 $/m^3 for PV-Battery supported. In line with the

analyses, it has been seen that the PV-Grid-Battery scenario is the most promising scenario. As a result of the study, it is proposed to examine the effect on water storage capacity and the overall cost of water evaporation while investigating the feasibility of combining RO with renewable energy. In addition, it was emphasized that with future studies, different tariff methods will be taken into account to sell surplus electricity to the grid.

2.2.2. Desalination with Wind Energy

Today, besides solar energy, wind energy is one of the most popular renewable energy sources used and analyzed in desalination technologies. Today, wind power is used to meet the electricity needs of an off-grid desalination plant. Wind energy integrated desalination systems are widely used especially in coastal and mountainous regions where wind energy is at its maximum potential. Desalination technologies using wind energy can be integrated into systems in different ways. Wind energy in desalination units can be used directly or indirectly in four different ways such as electricity, thermal, gravitational potential and kinetic energy (Ma and Lu 2011) . Wind energy is mainly used to power RO, ED desalination plants and steam compression VC and MVC distillation processes. An exemplary Wind-RO system consists of a wind generator, charge control equipment, battery, inverter and RO plant, as shown in Figure 11. The purpose of the Wind-RO system is to charge the batteries and provide the necessary power to operate the high pressure pumps. The battery group in the system maintains the balance in the power system and stores energy to be used in the absence of wind. The charge controller, on the other hand, provides controlled charging of the batteries. Table 6 shows the countries using wind powered desalination systems.

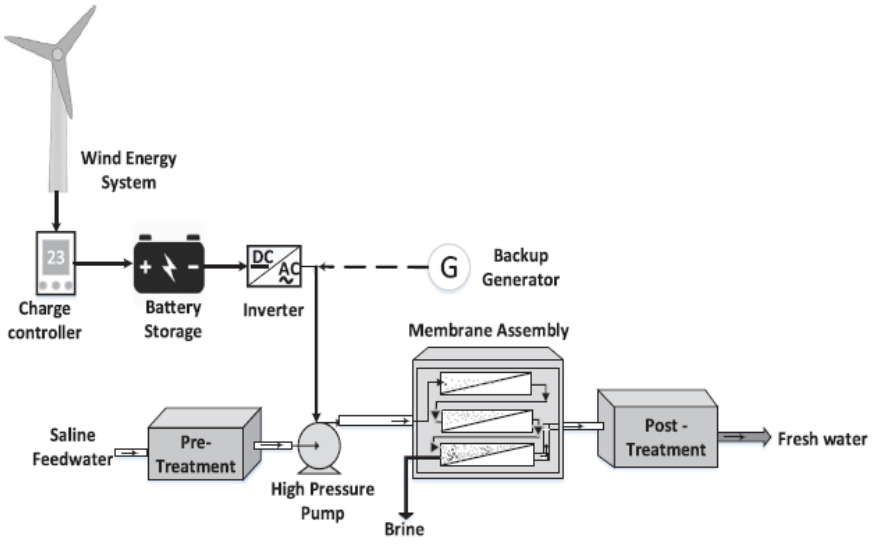

Figure 11. Wind-RO desalination unit (Khan, Rehman, and Al-Sulaiman 2018)

Table 6. Use of wind assisted desalination system in world countries (Abdelkareem et al. 2018; Ma and Lu 2011)

Country	**Feed Water Type**	**Fresh Water Extraction (l/h)**	**Specific Energy Consumption (kWh/m^3)**
France	Seawater - brackish water	500	4
UK	Seawater	500	2.5
Greece	Seawater	3300	30
Spain	Seawater	2333	225
Germany	Brackish water	250-370	6
Australia	Brackish water	5400	30
Enercon-Mediterranean	Seawater-brackish water	7.5-15	Seawater :2-2.8 / Brackish Water:0.8-1.3

Murat and Oznur (Gökçek and Gökçek 2016) conducted the technical and economic analysis of a desalination plant with wind energy and grid-supported reverse osmosis technology to produce clean drinking water in Gökçeada. The cost of domesticated water and electricity has been estimated for the production of clean water in Gökçeada. It is estimated that the production cost of water will be between 2,292 \$/m^3 and 6,457 \$/m^3 for all wind turbines and discount rates evaluated for the off-grid option. It is predicted that the production cost of water will be between 1,489 \$/m^3 and 1,750 \$/m^3 for different discount rates only in the system connected to the grid. In addition, the cost of water generation for a grid-connected system powered by a 30 kW wind turbine is projected to be between 0.866 \$/m^3 and 2,846 \$/m^3. It has been seen that the results of

the analysis are compatible with the literature and it has been stated that the production of drinking water supported by wind energy is economically feasible. It was emphasized that the study could be improved with the addition of energy recovery devices in the future.

Asensio et al (Rosales-Asensio et al. 2019) made an efficiency analysis of the wind power-assisted 5211 m^3/d capacity reverse osmosis desalination plant, which has been operating for more than 15 years, and suggested improvements to reduce the water production cost. The live data of the facility was used within the scope of efficiency analysis. An evaluation of the exploration costs was made by considering alternative configurations different from the existing ones in the study and it showed that two alternative proposed alternative systems could be advantageous in terms of cost of water (COW). These two configurations were determined assuming wind turbines with a nominal power of 2.64 MW providing the required energy. In both configurations, analyzes were made by adding energy recovery equipment and efficient pumps to the existing scheme. As a result of the analyzes made, it was seen that the water production cost decreased from 0.804 €/m^3 to 0.782 €/m^3. In addition, it has been calculated that it will provide a profitability index of 1.3794 in 10 years with an additional capital cost of 196000 €.

2.2.3. Desalination with Geothermal Energy

The use of geothermal energy is becoming more widespread throughout the world. Geothermal energy is used to produce heat and electricity. Geothermal energy reservoirs are divided into two according to their temperatures; Reservoirs with a temperature below 150^{o}C are divided into low-temperature reservoirs, and reservoirs at a temperature above 150^{o}C are divided into high-temperature reservoirs (Barbier 2002). Geothermal reservoirs produce steam and hot water. Geothermal energy has a serious use for thermal desalination processes such as MED, MSF, MD, VC and membrane desalination processes such as RO, EDR. In geothermal energy, the superheated steam coming out of the reservoir can easily be converted into heat and electrical energy, thus providing a more economical electricity production opportunity compared to traditional sources.

There is no need for thermal storage in the use of geothermal energy to power desalination plants. In addition, geothermal energy has a great advantage over wind and solar energy sources as the power output is constant (Bourouni, Tunisia, and Tunisia 2005). Reservoirs deeper than 100 m can be used to power desalination plants. Moreover, with the developments in membrane distillation technology, the use of geothermal brine with temperatures up to 60^{o}C has also become a solution. It has been determined that 24 countries produce electricity using geothermal energy and that five of these countries meet approximately 22% of their needs from geothermal energy (Fridleifsson et al. 2008). Table 7 shows the countries using geothermal energy in desalination systems.

Table 7. Studies of geothermal energy assisted desalination system (Abdelkareem et al. 2018)

Country	**Feed Water Type**	**Desalination Technologies**	**Fresh Water Capacity (m^3/d)**
Mexico	Seawater	MED-MSF	1
Greece	Brackish water	MED-MSF	80
Tunisia	Seawater	MD-MED	1382
USA	Seawater	MED-VTE	18.9
USA	Seawater	MED-VTE	79.5

In the first part of the study by Chekir (Chekir 2020), an overall evaluation of desalination technologies around the world and the latest developments in desalination technologies supported by renewable energy sources are presented. In the second part, traditional desalination technologies and facilities working with geothermal energy are examined and the appropriate system selection for Tunisia is provided. The geothermal potential of Southern Tunisia consists of thermal waters with temperatures ranging from 30 to 80°C. It has been determined that the technical characteristics of the wells in Tunisia will support the MED desalination technology. In addition, SWOT analysis has been carried out within the scope of the study, and it has been proven that geothermal energy is suitable for supplying fresh water to remote communities in Tunisia. Within the scope of the study, the cost of obtaining fresh water from 1 m^3 of brackish water using geothermal energy was calculated as 1.6 $. It has been emphasized that geothermal energy is suitable for continuous thermal desalination technologies if it has sufficient enthalpy.

Pietrasanta et al. (Pietrasanta et al. 2022) carried out the optimization study of the geothermal energy-assisted desalination system using a nonlinear optimization mathematical model. With this proposed model, the geothermal energy and desalination

systems were designed by using it as a simulator or an optimizer. This model selects the operating conditions and dimensions of selected processing units, such as multiple effect distillation (MED) or reverse osmosis (RO) subsystems for desalination and single flash (SF) or double flash (DF) geothermal powerplant (GPP) for electricity generation. aimed to obtain the optimal configuration. The optimization results showed that the optimal design was strongly dependent on the desired freshwater production levels. For freshwater production rates ranging from 200 to 800 kg/h, SFGPP and MED units were selected in the optimal configuration, and their total annual costs were found to vary between 15.63 and 20.85 M$/y. Then, the optimal configuration for 1000 kg/h was changed to an integrated system consisting of SFGPP, MED process, and RO units, and an energy recovery turbine (ERT) was used in this system. But in this case, the total cost increased to 25.66 M$/y. This last configuration was chosen as optimal for freshwater production rates ranging from 1200 to 1400 kg/h without ERT, with total annual costs ranging from 30.49 to 34.72 M$/y. Finally, the flexibility of the model allowed optimization of fixed configurations. For example, the lowest total annual cost for 1000 kg/h freshwater production was obtained by applying the geothermal/MED/RO (25.66 M$/y) configuration, followed by geothermal/MED (26.26 M$/y) and geothermal/RO (36.9 M$/y) has been observed to follow.

2.2.4. Desalination with Hybrid Energy Systems

Wind and solar energy are used separately from the grid or connected to the grid to generate electrical energy. However, due to the variable production potential, their yield is lower. Hybrid renewable power plants are simple to use, they meet the energy needs of the system by using different generation sources or storage systems in cases where one of the production sources is not available. An exemplary wind power and solar powered hybrid system is shown in Figure 12. As seen, the electricity consumed during the desalination process is supplied from PV and wind energy systems, and it is an integrated system with battery storage. During periods of intermittent production, stored energy is used to meet the electricity consumption.

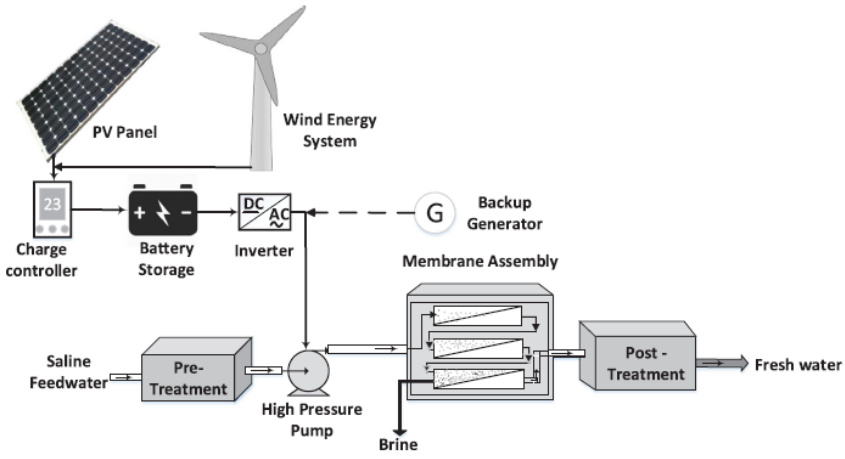

Figure 12. Diagram of hybrid PV-Wind assisted desalination system (Khan, Rehman, and Al-Sulaiman 2018)

Atallah et al. (Atallah et al. 2020) proposed a desalination system with hybrid energy-assisted reverse osmosis technology to produce 100 m^3 of fresh water per day in Nakhl, Egypt. 11 different energy systems such as diesel, PV, wind turbine, and battery were used to select the optimum configuration and economical sizing for the RO plant. The energy systems examined are a stand-alone diesel system with and without a storage battery, a photovoltaic panel system with a storage battery, a wind turbine system with a storage battery, a hybrid diesel/PV system with a storage battery, a hybrid diesel/wind system with and without a storage battery, a storage battery. It is a PV/wind system with a PV/wind system and a hybrid PV/wind/diesel system with a storage battery. The system to be created is based on the analysis of three basic factors such as economic, technical, and environmental trends. 11 different energy system scenarios were simulated using the HOMER program. As a result of the simulations, the 6th system, i.e. PV/diesel/battery hybrid system, was determined as the optimal system for the RO facility in Nahkl, Egypt. 6th system consists of a 160 kW PV panel, a 50 kW fixed capacity diesel generator, 190 lead-acid batteries, and a 39.3 kW inverter. With this system, it has been observed that carbon dioxide (CO_2) gases are reduced by approximately 94%. The renewable rate (RF) of the 6th system is 93.1%, it is stated that it can help to overcome the problem of lack of electricity grid in remote and arid regions. It was emphasized that the system meets 100% of the demanded energy and there will be no capacity shortage. It has also been stated that the stability and safety of the electrical system will increase by storing the excess electricity in this system in batteries. The project cost of the PV/diesel/battery hybrid

system was calculated as 502,661.50 $, while the energy cost was calculated as 0.1074 $/kW.

Eltamaly et al. (Eltamaly et al. 2021) proposed a desalination plant design with hybrid energy assisted reverse osmosis technology with a capacity of 1000 m^3/d for obtaining fresh water in remote areas in Saudi Arabia. The proposed hybrid system consists of wind turbines, photovoltaic panels and a battery pack. The energy requirement for this hybrid system to produce 1000 m^3/d of fresh water is calculated as 2440 kW. For the optimization of the hybrid system; Three different optimizations were used, namely particle swarm optimization, bat algorithm, and social imitation optimization. As a result of the optimization analysis, it has been determined that this hybrid system is the most optimum design for Arar City. In addition, the freshwater production cost of the hybrid system was calculated as 0.75 $/$m^3$.

Gomaa et al. (Gomaa et al. 2023) examined hybrid renewable energy systems using Homer software to select the most suitable scenario for meeting the energy demand of a 12000 m^3/d capacity desalination plant with reverse osmosis technology. Scope of work; Diesel generator, Diesel Generator-Battery, Wind-Diesel generator, Wind-Diesel Generator-Battery, Photovoltaic (PV)-Diesel generator, PV-Diesel Generator-Battery-Wind-Diesel generator, PV-Wind-Diesel Generator-Battery, Wind -Fuel Cell-Diesel generator, Wind Fuel Cell-Diesel Generator-Battery, PV-Fuel cell, PV-Fuel Cell-Diesel generator, PV-Wind-Fuel cell, 12 different systems were examined. According to the results of the economically compared hybrid systems analysis, the most suitable hybrid power system configuration was determined as the system containing PV-Wind-Diesel Generator-Battery. In the PV-Wind-Diesel Generator-Battery system, 1000 kW PV Panel, 1000 kW diesel generator, 1750 kW battery and 1500 kW inverter were used. The annual capacity of this system is 22,214,414 kWh, the energy cost is 0.063 $/kWh and the annual CO_2 emission is 445221 kg.

CHAPTER 3

MATERIALS AND METHODS

A desalination system has been established for the desalination of geothermal brine with a temperature range of 50-550 °C, taken directly from the re-injection lines at the Yenikale geothermal heat center in Yenikale, Izmir. This water desalination system and it's PV system are shown in Figure 13. The system includes a membrane, low and high- pressure pumps, a dosing pump, valves, a sand a filter and a tank where geothermal water is stored. The electricity consumption of the pumps is provided by solar energy, using 12 PV panels of which has a capacity of 320 W each. The spent water is kept in tanks and sent to the sand filters to reduce sediment and turbidity before being desalinated by the membranes.

Figure 13. Reverse osmosis and PV systems of the geothermal heat center in Yenikale (Tomaszewska et al. 2021)

The PV production values and desalination consumption values in the current desalination system are given in Table 8.

Table 8. Desalination consumption – PV production values for existing system (TUBITAK-NCBR 2022)

Date-Hour	Desalination Consumption (W)	PV Production (W)
03.09.20 - 14:05	1370	2701
03.09.20 - 14:20	1369	2698
03.09.20 - 14:36	1372	2674
03.09.20 - 15:07	1373	2537
03.09.20 - 15:22	1380	2487
29.09.20-10:10	1407	1277
29.09.20-10:25	1412	1458
29.09.20-10:40	1407	1550
29.09.20-11:10	1414	1950
29.09.20-11:40	1408	2287
28.10.20-10:05	1462	903
28.10.20-10:21	1463	805
28.10.20-10:36	1477	438
28.10.20-10:51	1456	791
17.11.20-09:12	1436	126
17.11.20-09:27	1437	144
17.11.20-09:57	1442	173
17.11.20-10:42	1438	230
17.11.20-11:12	1430	268
17.11.20-12:07	1436	249
17.11.20-12:22	1432	239
17.11.20-12:52	1423	217

The present study has focused on improving the existing solar energy supported desalination system to reduce grid usage and use PV electricity generation at its maximum level. In this regard, a battery has been added to store excess energy produced during times of high PV production and to be used on days when production is not possible. The schematic of the modified system with the battery is shown in Figure 14.

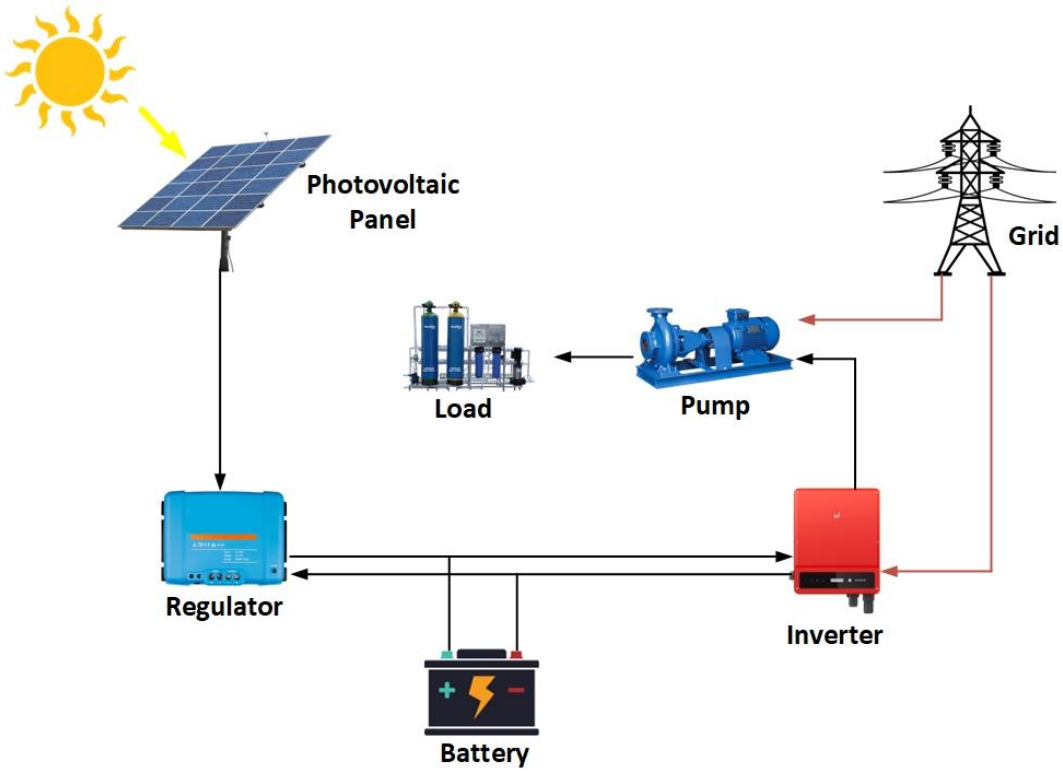

Figure 14. Battery integrated PV system

In the proposed system, the desalination system consumption is considered as a constant load and is provided by the panels during the day. As seen in Figure 15, battery and grid support are used at times when there is no production from panels or there is insufficient production. For a battery to be used sufficiently, it must be charged at certain times. In cases where panel production is high, the battery is charged to its discharge capacity and then the desalination load is met. However, when there is insufficient production in the panels, the load is met by the battery if the battery is capable of discharging. But if the battery is empty, the battery is charged first, and a constant load of 1450 W is provided from the grid during daylight hours.

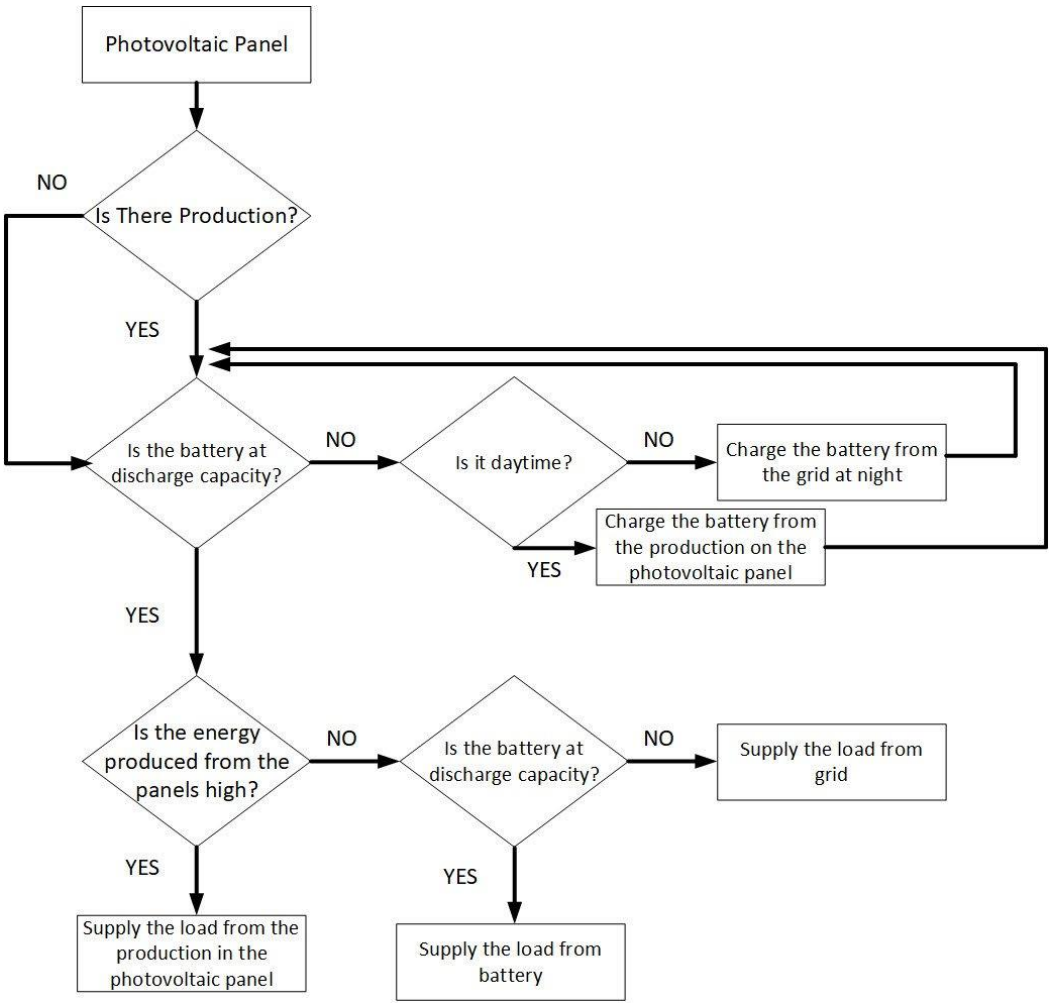

Figure 15. The working principle of proposed improved system

The TRNSYS illustration of the proposed system which shows the stream flows of the unit, is depicted in Figure 16. As can be seen that, there are different components (types) in this flow diagram and their introduction and explanation are presented in Table 9.

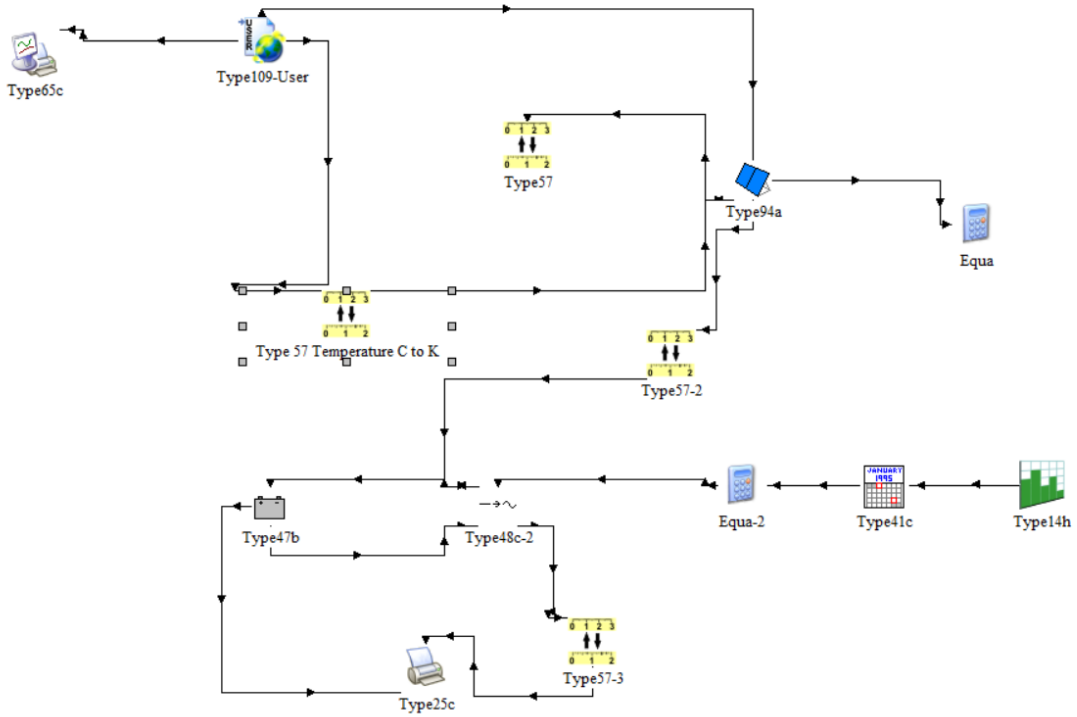

Figure 16. The TRNSYS illustration of the proposed system

Table 9. Description of system components in TRNSYS

Component	Type	Description
The weather component	109	This component, calls the weather data component, allows us to access weather data at intervals for the desired region. It helps us to obtain weather data such as solar radiation, wind speed, humidity rate.
Unit conversion unit	57	This component is used to convert the unit of the results obtained into the units required for the components.
Load profile	14-41	Type 14 is used to determine the daily power consumption.
Crystalline solar panel	94	Type 94 is used for photovoltaic panels and models the electrical performance of the panel.
Battery	47	The Type 47, which is used as a lead acid battery, works in connection with PV panels and power conditioning components.
Inverter	48	It models two power conditioning devices used in photovoltaic systems, called inverters and regulators.
Printer	25	These components have been used to display the desired values during the simulation.
Online plotter	65	

3.1. Methodology

In this section, the evaluation of the proposed system is presented in more detail. As mentioned earlier, this system is designed to improve the performance of the existing system at the Yenikale geothermal heat center in Yenikale, Izmir. The details of the modeling of this system is shown in Figure 17. In this study, PV panels and battery storage system were modeled and simulated using TRNSYS software under three different scenarios. The goal of the study was to determine the most suitable component designs that would minimize waste and reduce reliance on the grid by maximizing the use of solar energy. After obtaining results from the simulations, an exergo-economic analysis was conducted using the EXCEM method.

Modeling of the proposed system has been done using TRNSYS software. The characteristics of the equipment used in the relevant system have been defined to the components included in TRNSYS' own structure, and the results of the desired values have been obtained. TRNSYS is a simulation program for renewable energy systems that is known for its accuracy and flexibility. Its key feature is capability of modeling complex systems with time-dependent functions, which makes the software a powerful tool for simulating various renewable energy systems. It has an accuracy rate of 99.8% compared to other simulation programs (Racquel Lovelace 2015). The outputs in the study are hourly values for one year. Due to the large number of data, energy, exergy and economic calculations were made with Excel. Excel is a versatile tool for performing complex mathematical calculations and enables users to easily visualize and store their results. Moreover, it is ideal for analyzing and processing data, as well as reorganizing, adding, or modifying previous operations.

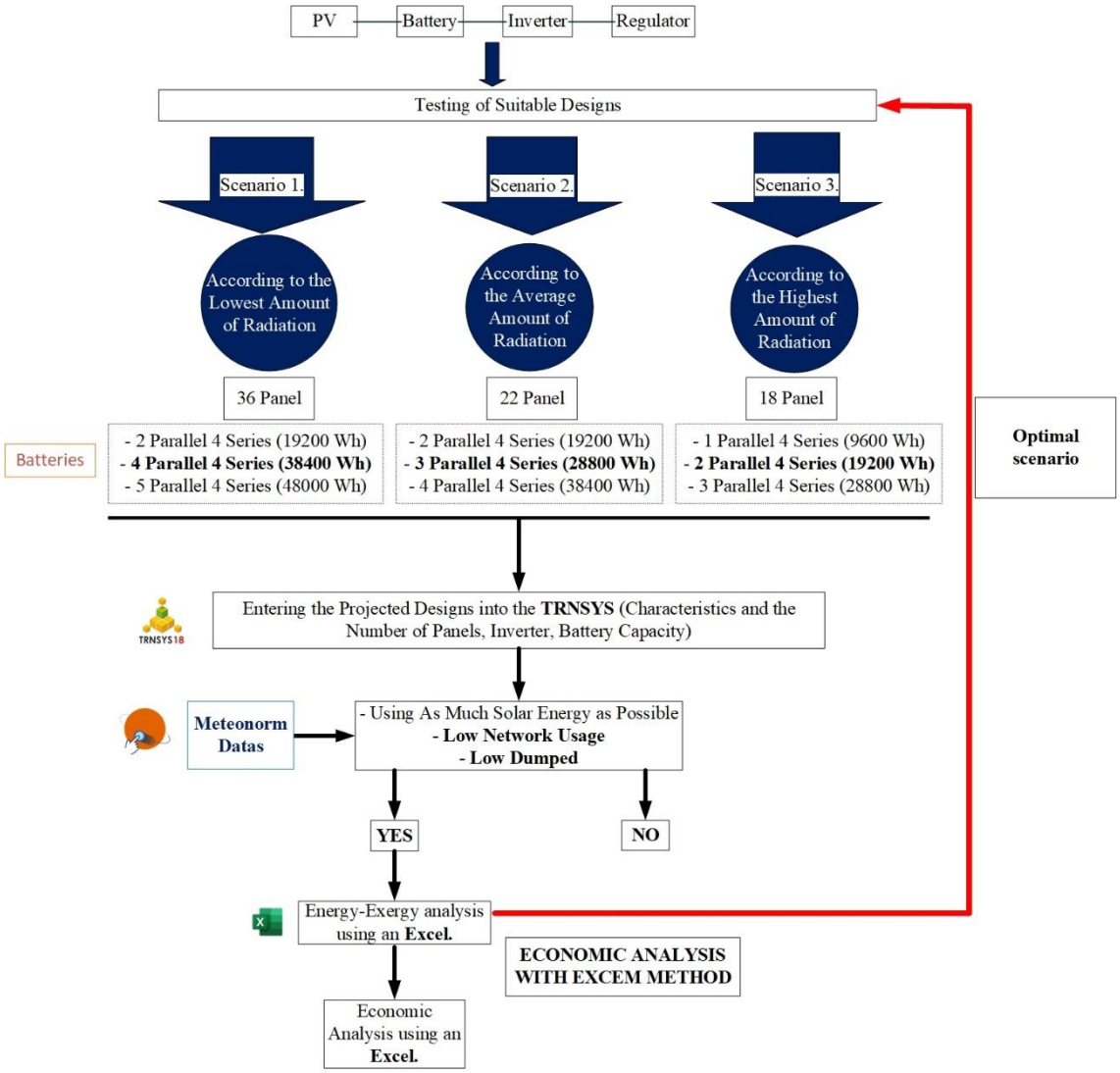

Figure 17. The flow diagram of the proposed system modeling

3.2. Modeling Assumptions

When modeling and evaluating the system, it is essential to make certain assumptions to simplify the analysis. In this section, the assumptions made in the proposed system model and analysis are provided.

The proposed system's assessments rely on the first and second laws of thermodynamics. While considering simplifying assumptions including open system and steady state conditions, these laws are expressed as follows (Srivastava 2013):

$$En_{in} = En_{out} \quad (1)$$

$$Ex_{in} - Ex_{out} = Ex_{loss} \quad (2)$$

Here, Ex_{in} represents the inlet exergy, and according to the Petela equation (Petela 2008), it only represents solar radiation. Also, Ex_{out} represents the maximum output exergy extracted from solar radiation.

The PV and battery storage system was designed for three different scenarios with varying environmental conditions. The number of PV panels and battery capacity required for each scenario were determined, and the results were analyzed parametrically. PV panel and battery calculations were performed according to 3 different scenarios. The parallel and serial calculations based on the battery inverters were calculated according to the characteristics of inverter and regulator. The formulations used for the calculations of PV panels and batteries specified in the scenarios are provided in the energy analysis section of the methodology.

The scenarios are considered as follows:

- Scenario 1: The system has been designed according to the lowest radiation. 36 panels with a power of 320 W were used and the battery capacity was determined as 38400 Wh.
- Scenario 2: The system was designed according to the average radiation while it was being designed. 22 panels with a power of 320 W and a battery capacity of 28800 Wh were used.
- Scenario 3: The panel and storage capacity were selected according to the highest radiation. 18 panels with a power of 320 W and 19200 Wh storage are designed.

The radiation data for the Yenikale Geothermal Heating Center located in the Dikili district of Izmir was obtained from Meteonorm, providing the daily amount of radiation per unit area for the year 2021, which offered the most up-to-date information. To determine the highest radiation value, the average radiation values for the months of July and August were considered. For the lowest radiation value, the average radiation values for the months of December and January were used. Lastly, to find the average radiation, data from the entire year was taken into account. The recorded values were as follows: For the lowest radiation, it was 3149.068 W/m²day, for the highest radiation, it was 7788.63 W/m²day, and for the average radiation, it was 5806.0956 W/m²day.

The modeling of the PV panels, regulator and inverter involves certain assumptions regarding their characteristics. The technical specifications of the 320 W rated PV panels used in the system are provided in Table 10. The inverter is a crucial component that converts DC power generated by the panels into usable AC power. A regulator is also included in the system design to prevent overcharging of the battery. The GW-5000DT inverter with a capacity of 5 kW was utilized in the current system, as depicted in Figure 16.

The regulator and inverter efficiencies were assumed to be 78% and 98%, respectively, based on their datasheets. These values were specified in the relevant section where data for components is entered in TRNSYS. As a result, the losses in battery charging and the DC/AC losses conversion in the inverter were taken into account in the obtained outputs after modeling. Figure 18 shows the general system diagram of the regulator, inverter, and battery.

Table 10. Technical specifications of the panel (HT-SAAE 2020)

Model	**HT-SAAE HT60-156M**
Max power at STC (P_{max})	320W
Optimum operating voltage/rated voltage (V_{mp})	34.4V
Optimum operating current/rated current (I_{mp})	9.33A
Open-circuit voltage (V_{oc})	40.7V
Short circuit current (I_{oc})	9.99A
Normal operating cell temperature (NOCT)	45C
Dimensions	1640X992X35 mm (1.63 m^2)
Weight	18.5 kg
Number of cells	60

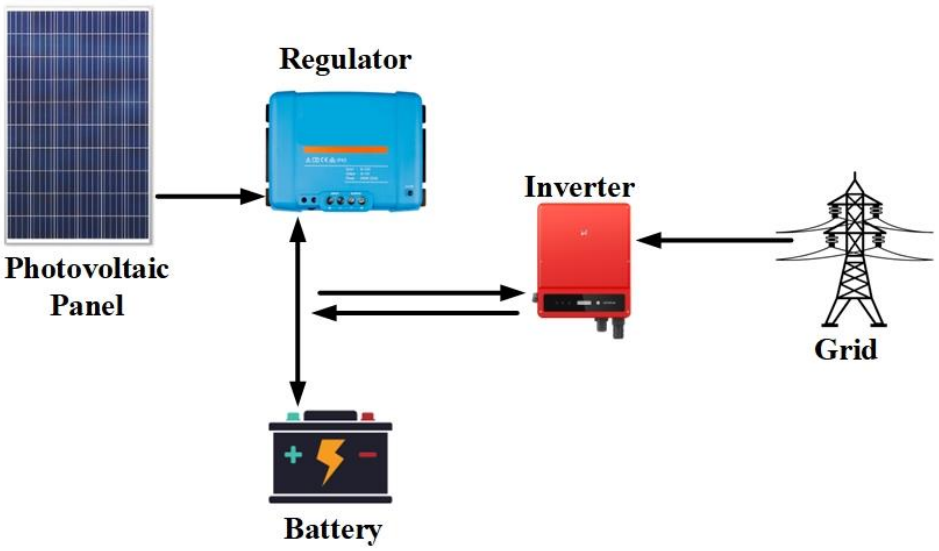

Figure 18. Schematic system design for inverter, battery and regulator

In addition, the existing system includes the utilization of the DG12-200 12V200AH RITAR battery. The technical data for the battery bank is given in Table 11.

Table 11. Technical specifications of the battery (Ritar Power 2020)

Model	**RITAR DG12-200(12V200Ah)**
Cells per unit	6
Voltage per unit	2V
Capacity	200Ah @20 hr rate to 1.75V @25 °C
Max discharge current	200 A (5sec)
Max charging current	40 A

By analyzing the battery datasheet, it can be observed that there is a correlation between the depth of discharge (DOD) and the number of cycles. Specifically, when the battery is discharged to 50% of its capacity, it can undergo approximately 1500 charge-discharge cycles. This implies that the battery's lifespan is extended when operated at a 50% depth of discharge. In simpler terms, as the depth of discharge increases, the number of cycles decreases. Hence, in order to optimize battery longevity, the batteries were utilized with a 50% depth of discharge. The number of cycles according to depth of discharge is shown in Figure 19.

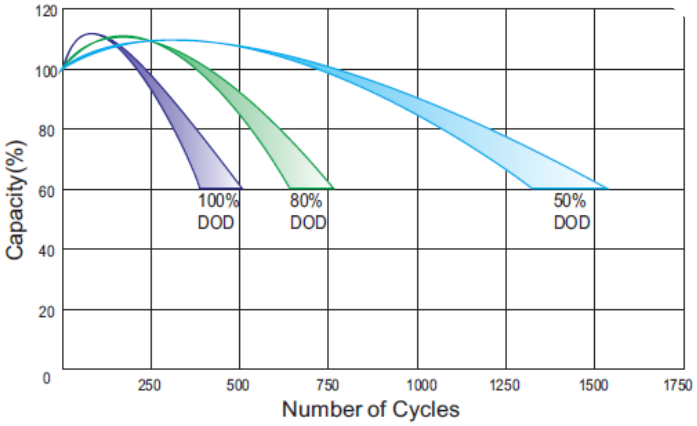

Figure 19. Cycle life and depth of discharge (Ritar Power 2020)

3.3. Energy Analysis

In this section, equations related to the components of the proposed PV-battery system were provided, and the energy analysis of the system was carried out. The components of the system described in the new system proposal section and schematized in Figure 14 are indicated below.

When sizing PV panels, the first step is to determine the maximum power that can be obtained from the PVs. The maximum panel power is a parameter dependent on the panel efficiency, the panel area used, and solar radiation, it is calculated as (Abdul Ghafoor and Munir 2015; Marwan M. Mahmoud and Ibrik 2006):

$$PV_{MPP} = 1000 \cdot \eta_{FV} \cdot A_{FV} \tag{3}$$

where, η_{FV} , A_{FV} , and 1000 refer to the photovoltaic panel efficiency, the photovoltaic panel area, the solar radiation, respectively.

The radiation amount per unit area, daily energy requirement, and total system efficiency must be determined to calculate panel area. The ratio of the daily energy requirement to the multiplying of the total system efficiency and the radiation amount per unit area gives the required panel area. The photovoltaic panel (A_{FV}) area is expressed as below (Marwan M. Mahmoud and Ibrik 2006; Padmavathi and Daniel 2013):

$$A_{FV} = E_{LD}/(\eta_s \cdot E_{SD}) \quad (4)$$

where, E_{LD} , η_s , and E_{SD} denotes to the daily energy requirement (Wh/day), the total system efficiency, and the daily amount of radiation per unit area (Wh/m^2day), respectively.

The total system efficiency in the above equation is defined as (Padmavathi and Daniel 2013; Marwan M. Mahmoud and Ibrik 2006):

$$\eta_s = \eta_{FV} \cdot \eta_{PCU} \cdot \eta_o \quad (5)$$

where, η_{FV}, η_{PCU} , η_o correspond to the efficiency of the photovoltaic panel, efficiency of the inverter, the cable, temperature effect and other losses.

Batteries are used for energy storage or backup when there is no sunlight during certain times of the day. Excess production from the solar panels during peak times is used to charge the battery. The stored energy in the battery is then transferred to the load during non-production times. The battery capacity is as below (Fairuz et al. 2023):

$$E_{battery} = \frac{E_{LD} \cdot n}{DOD \cdot \eta_b \cdot v} \quad (6)$$

Here, E_{LD}, n, DOD, η_b, and v contribute the daily load profile, the number of autonomy days, the depth of discharge, the battery efficiency and the system voltage.

In this study, different battery capacities were tested to use as much solar energy as possible and the least grid electricity. Three different battery capacities have been determined for the lowest radiation, highest radiation and average radiation scenarios. Among them, energy-exergy analysis and economic analysis were performed for the battery capacity that gives the most optimal value.

For energy performance evaluation the efficiency of converting solar radiation into electricity by PV panels is defined. This criteria can be expressed as the ratio between the electrical output energy and the solar radiation input exergy (Duran Sahin, Dincer, and Rosen 2007):

$$\eta = \frac{E_{gen}}{S_t \cdot A} \tag{7}$$

Here, E_{gen} refers to the electric generation from PV panels, S_t (W/m^2) refers the solar irradiance and $A_{PV}(m^2)$ refers PV area. Also, the electricity generated from PV panels is calculated by multiplying the current and voltage at the maximum power point:

$$E_{gen} = V_{MP} \cdot I_{MP} \tag{8}$$

V_{MP} and I_{MP} expressions refer to the maximum operating voltage and current order.

3.4. Exergy Analysis

Exergy analysis is a thermodynamic methodology used to determine the quality of energy in a system. Exergy is the maximum amount of work that can be obtained from a system when it reaches equilibrium with its surroundings (Luis and Van der Bruggen 2014). Exergy analysis evaluates the destruction and losses of exergy within a system, allowing the identification of the sources of inefficiencies and the potential for improvement in the system's performance. In this section, an exergy analysis has been conducted, taking into account exergy destruction.

The exergy analysis of PV panel can be explained with the following equation (Srivastava 2013)

$$\text{Exergy Input} = \text{Exergy Output} + \text{Exergy Loss} + \text{Irreversibility} \tag{9}$$

The degradation in the quality of exergy is called exergy loss, or in other words, irreversibility (Hepbasli 2008).

The input exergy of the PV system, which is related to the radiation intensity, refers to the solar power obtained from the solar modules (Ghanim, Fowzi, and Obaid 2019)

$$E_{x,solir} = A \cdot S_t \left(1 - \frac{T_{amb}}{T_{sun}}\right) \tag{10}$$

Here, S_t (W/m^2) , $A_{PV}(m^2)$, T_{amb} (K), and T_{sun} (K) refer to the solar irradiance, PV area, ambient temperature, and suns temperature, respectively.

To determine the exergy output of a photovoltaic system, one can calculate the outlet exergy that consists of both thermal and electrical exergies. The thermal exergy is associated with the heat energy released by the system, while the electrical exergy is associated with the electrical energy generated by the system. The total exergy output of a PV system is the sum of these (Yazdanpanahi, Sarhaddi, and Mahdavi Adeli 2015; Srivastava 2013):

$$EX_{out} = EX_{electrical} + EX_{thermal} \tag{11}$$

Electrical exergy equal to PV panel production value (Rawat, Lamba, and Kaushik 2017):

$$EX_{electrical} = V_{OC} \cdot I_{SC} = V_{MP} \cdot I_{MP} \tag{12}$$

Here, V_{MP} and I_{MP} expressions refer to the maximum operating voltage and current order.

Thermal exergy, which is associated with the panel area, ambient temperature and module temperature, is the heat loss from the panel surface to the environment (Sarhaddi et al. 2009; Srivastava 2013):

$$EX_{thermal} = UA_a(T_{amb} - T_m) \cdot \left(1 - \frac{T_{amb}}{T_m}\right) \tag{13}$$

where, the U value is the general heat loss coefficient by means of convection for a PV panel. The T_{amb} and T_m temperatures are the ambient temperature and the PV module temperature, respectively.

The convective heat transfer coefficient, which is related to the overall heat loss coefficient, is calculated as follows (Duran Sahin, Dincer, and Rosen 2007; Ghanim, Fowzi, and Obaid 2019):

$$h_{conv} = 2.8 + 3V_w \tag{14}$$

where, V_w refers to the wind speed.

The exergy efficiency of PV panels is the ratio of the output exergy to the solar radiation exergy, which is characterized as the input exergy (Duran Sahin, Dincer, and Rosen 2007):

$$\psi = \frac{Ex_{out}}{E_{x,solir}} \tag{15}$$

3.5. Exergo-economic Analysis

Exergo-economic analysis is an evaluation that includes exergy and economic aspects together. The general equation that was considered to implement this analysis on the proposed system is as follows (Razi, Dincer, and Gabriel 2020):

$$\text{Input Cost} + \text{Generated Cost} - \text{Output Cost} = \text{Accumulated Cost} \tag{16}$$

In this equation the cost generation is defined as the sum of the capital price of the equipment and the maintenance and repair costs (Razi, Dincer, and Gabriel 2020):

$$\begin{aligned}\text{Cost Generation} \\ = \text{Capital Cost of Equipment} + \text{Other Creation and Maintenance Costs}\end{aligned} \tag{17}$$

Among the specified costs, only the capital cost was evaluated. Because the results of the generation cost are proportional to the cost of capital. Thus, the values will be compatible with each other.

If the capital cost of the system is represented by K, then the R value is obtained by dividing the exergy loss ratios by the capital cost (Razi, Dincer, and Gabriel 2020):

$$\dot{R} = L/K \tag{18}$$

The R parameter can be defined according to the energy loss rate and the exergy loss rate as below:

$$\dot{R}_{en} = \dot{L}_{en}/\mathrm{K} \tag{19}$$

$$\dot{R}_{ex} = \dot{L}_{ex}/\mathrm{K} \tag{20}$$

In the above equations, L refers to loss ratio. There are two thermodynamic loss rates, namely energy and exergy loss ratios. These mentioned loss rates are calculated using energy and exergy balance equations. The energy loss ratio ($\dot{L}_{en}$) is proportional to the waste energy output, and exergy loss ratio ($\dot{L}_{ex}$) is proportional to the waste exergy output and exergy consumption, which is caused by irreversibilities. The energy and exergy loss ratios are calculated as (Razi, Dincer, and Gabriel 2020):

$$\dot{L}_{ex} = \sum_{inputs} exergy\ flow\ rates - \sum_{outputs} exergy\ flow\ rates \tag{21}$$

$$\dot{L}_{en} = \sum_{inputs} energy\ flow\ rates - \sum_{outputs} energy\ flow\ rates \tag{22}$$

In addition to these, some parameters were also calculated to evaluate the system from an economic point of view. Net present value (NPV), payback period (PP), and cost of energy (COE) are the parameters that considered for economic assessments.

The NPV represents the overall profit earned throughout the project's duration and is expressed as (Bellos et al. 2019; Tzivanidis, Bellos, and Antonopoulos 2016):

$$NPV = -C_0 + CF\left[\frac{(1+r)^N - 1}{r(1+r)^N}\right] \tag{23}$$

where C_0 and CF refer to the investment cost of component and annual income cash flow.

Also, N is the project lifetime, and r is the discount rate which is considered as %3. The annual income cash flow is defined as follows: (Tzivanidis, Bellos, and Antonopoulos 2016; Bellos et al. 2019; Talebizadehsardari et al. 2020).

$$CF = k_{electrical} Y_{electrical} \tag{24}$$

where, Y is the energy parameter and k is the product cost.

The Payback Period indicates the duration for a company to recover its investment. Therefore, unlike NPV, which is affected by the lifetime of the project and the discount factor, it is only affected by the discount factor. The following equation is

used to calculate the payback period (Bellos et al. 2019; Tzivanidis, Bellos, and Antonopoulos 2016):

$$PP = \frac{ln\left[\frac{CF}{CF - rC_o}\right]}{\ln(1-r)} \tag{25}$$

The COE, which describes the cost of the energy produced by the solar during the lifetime of the system, is expressed as (Tzivanidis, Bellos, and Antonopoulos 2016; Bellos et al. 2019):

$$\mathrm{COE} = \frac{C_{PV}}{E_{tot}} \tag{26}$$

where, C_{PV} and E_{tot} (kWh/year) indicate the cost of installing a PV system and overall annual energy production.

3.6. Case Study

The location of the proposed system is in Yenikale, Izmir Türkiye. The geographical information of the region is given in Table 12. The location information of Yenikale is shown on the map in Figure 20.

Table 12. Geographical features of Yenikale, Izmir (Map TR 2023)

Province	Izmir
Latitude	38.4127°
Longtitude	27.1384°
Climate zone	Mediterranean

Figure 20. The location of Yenikale Heat Center, Izmir-Türkiye

The ambient temperature changes, wind speed distributions, and solar radiation variation during the year are given in Figures 21-23 respectively. As can be seen in Figure 21, the highest ambient temperature in the region is observed as 40°C in August, while the lowest temperature is observed as -3.04°C in December. According to the distribution of the wind data given in Figure 22, the lowest wind speed is determined as 0.5 m/s and the highest wind speed is determined as 14 m/s. The highest solar radiation was observed in June, July and the lowest solar radiation in December.

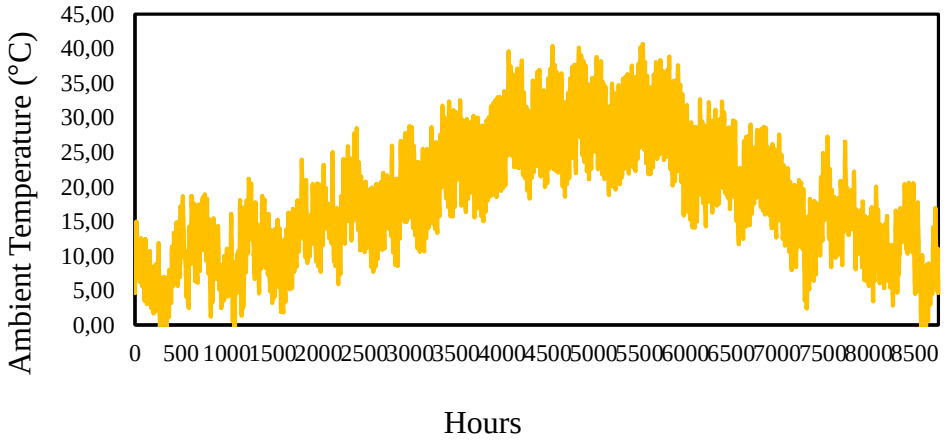

Figure 21. The hourly temperature variations (^{o}C)

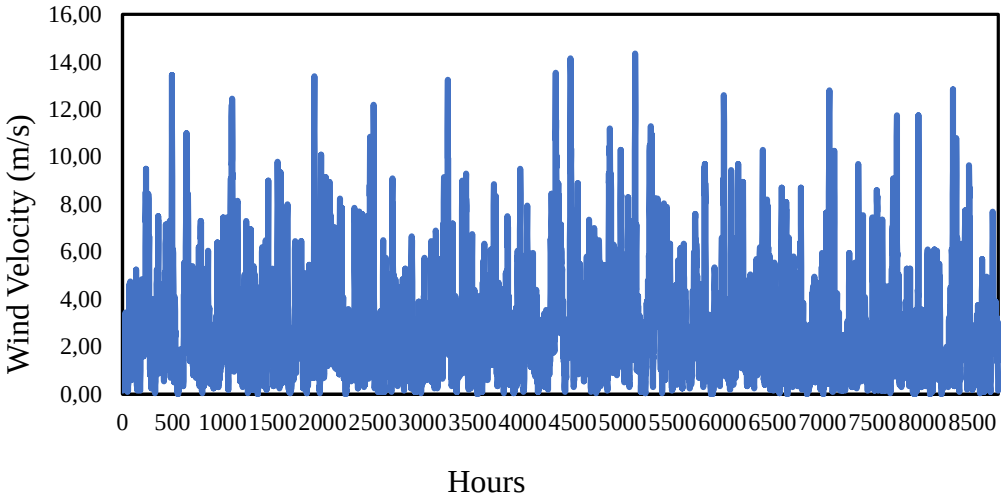

Figure 22. The hourly wind velocity distribution (m/s)

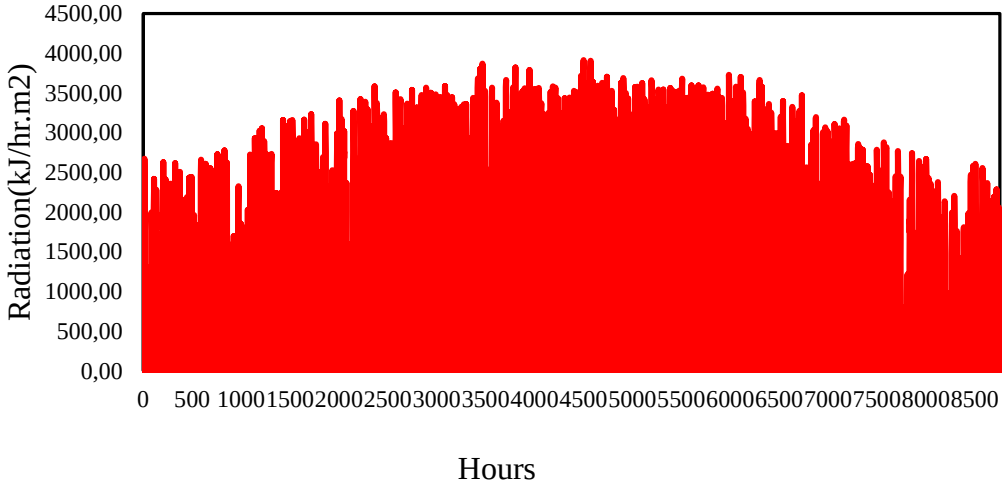

Figure 23. The hourly solar radiation (kJ/h.m^2)

CHAPTER 4

RESULTS AND DISCUSSION

In this section, the behavior of the proposed PV-battery-supported system, including the characteristics of the equipment used, particularly the battery's behavior, and the results of PV generation values, were examined. The system was adapted to three different scenarios based on the lowest radiation, average radiation, and highest radiation conditions. Energy and exergy analyses were conducted, and comparisons were made among them. Additionally, the economic parameters between the scenarios were specified.

4.1. Battery Charge-Discharge

The battery has been incorporated into the system to store excess PV generation during periods of high production. This allows for charging the battery and subsequently utilizing the stored energy during times when the PV generation is insufficient to meet the load demand. The charging and discharging powers of the battery have been analyzed in conjunction with the PV generation values.

The total charge-discharge powers of the battery and PV generation values by month are given in Figures. 24-26. for the lowest radiation, average radiation and highest radiation. When the solar panel production curve and battery charging curves were examined, the batteries were charged from the grid, not from the production on the panels, especially since there is insufficient production in the winter months. In the lowest radiation scenario, the grid usage is higher in battery charging because more batteries are used in addition to the less production.

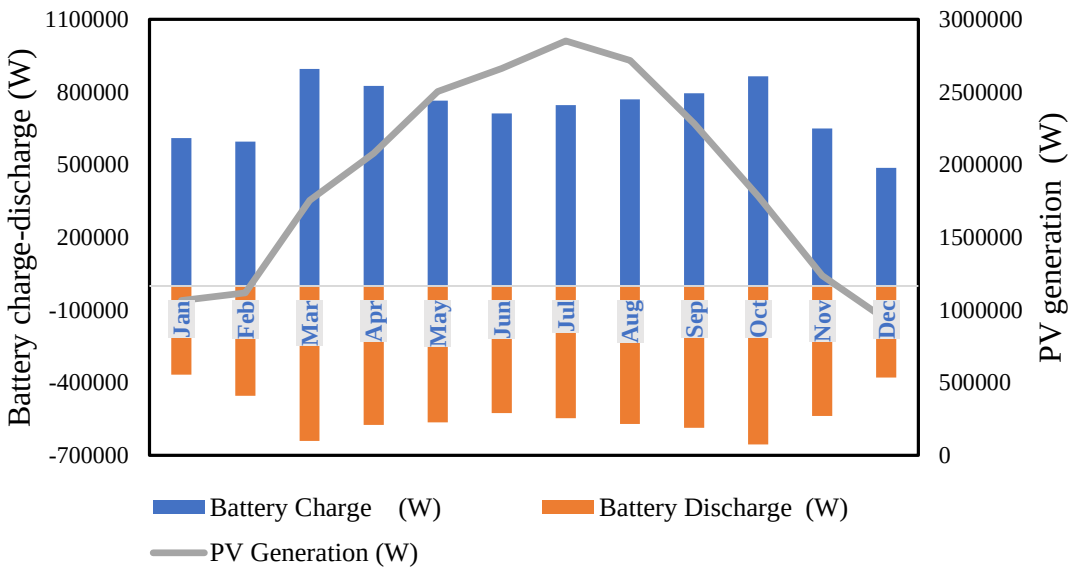

Figure 24. Battery charge-discharge/PV power for lowest radiation

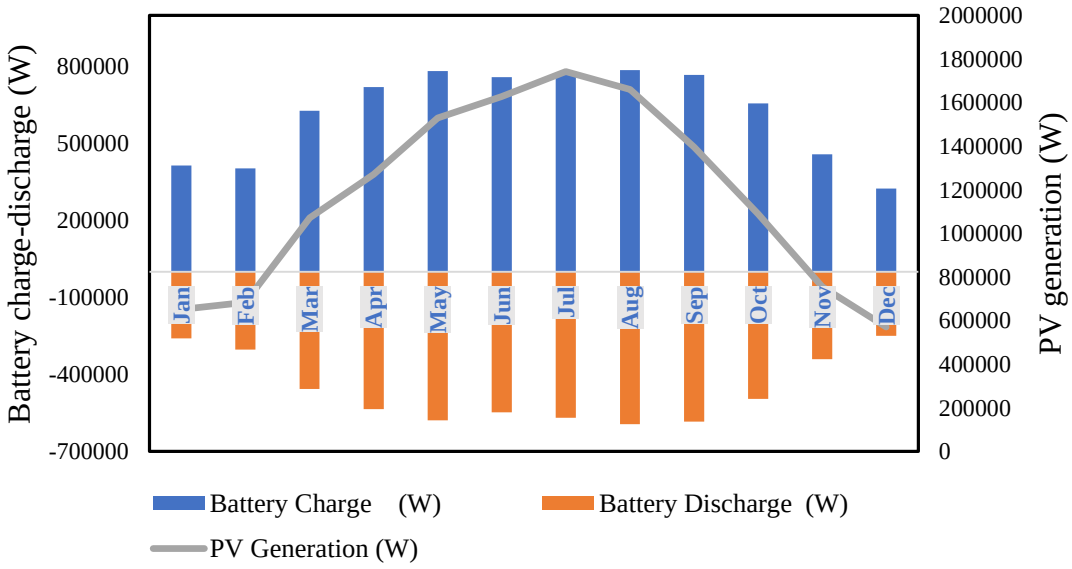

Figure 25. Battery charge-discharge/PV power for average radiation

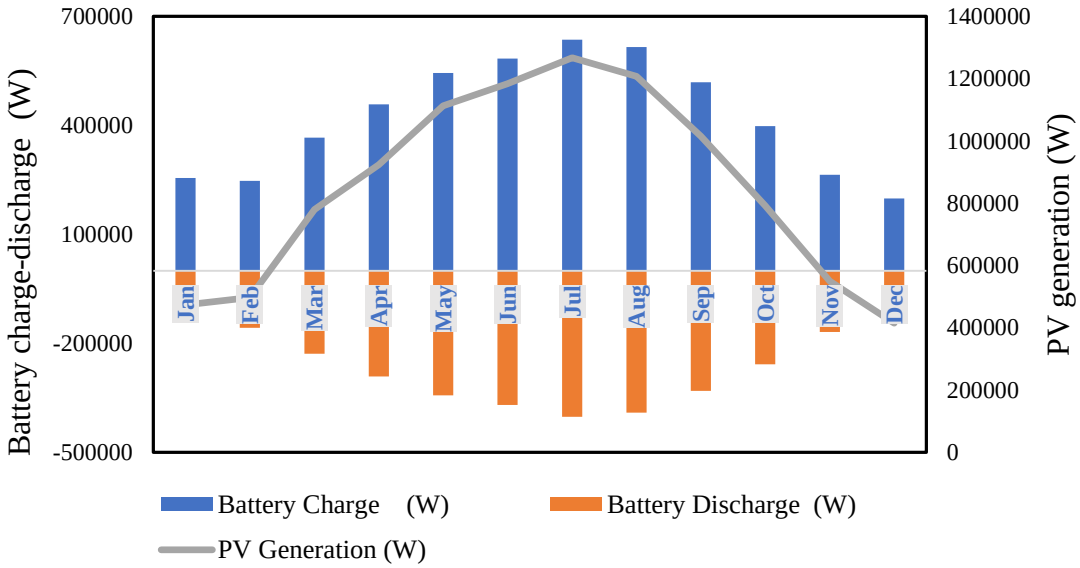

Figure 26. Battery charge-discharge/PV power for highest radiation

Battery Depth of Discharge

As mentioned in the modeling assumptions, a battery depth of discharge (DOD) of 50% was used. Battery manufacturers recommend not going below a 50% DOD. However, in this section, an investigation has also been conducted for using a 70% DOD for the battery. The discharge of the battery for supplying the load, utilization of PV generation, and grid usage have been presented for both 70% and 50% DOD levels. Additionally, the amount of energy that cannot be used for either charging the battery or supplying the load when PV generation exceeds demand (referred to as "dumped" energy) has been shown in these analyses. A comparison has been conducted as an example for a scenario with the average radiation value among system models based on scenarios with the lowest radiation value, the average radiation value, and the highest radiation value.

Table 13 . Different DOD values for battery

(kW)	50% DOD	70% DOD
Grid usage	3960.79	4041.26
PV production	14052.30	14052.30
Battery to load	5509.27	5740.69
PV to load	3239.61	2927.71
PV to battery	10740.55	11052.44
Grid to battery	7.68	7.68
Grid to load	3953.11	4033.58
Dumped	72.13	70.96

In the table 13, comparisons are provided for %70 and %50 Depth of Discharge (DOD) values.

1- The first evaluation parameter indicates that as the DOD value increases, the battery cycle count will also decrease. This implies that the battery will be used for a shorter lifespan.
2- Secondly, due to the decrease in battery cycle counts and consequently reduced usage life, the battery cost will increase.
3- When the values are examined, it can be observed that grid usage increases for the %70 Depth of Discharge (DOD) value. Since the battery is discharged more deeply, more energy is required to recharge it. At this point, the photovoltaic system will be utilized more to recharge the battery, but after a while, it becomes insufficient to supply the load, leading to an increase in grid usage.
4- The share of battery usage in supplying the load has increased.
5- Another parameter that needs to be considered is component losses. Deeper discharging of the battery requires more frequent recharging, leading to losses in the components during the charging process, which makes the system less efficient.

4.2. Energy-Exergy Analysis

Figures 27-29 present the production values of solar panels for the lowest, average, and highest radiation scenarios. When comparing the production values, it is observed that the highest production is achieved in the lowest radiation scenario, while the lowest production is observed in the highest radiation scenario, due to the number of panels used. As the number of panels increases, the production quantity also increases.

In addition to the number of panels, changes in solar radiation intensity also affect PV panel production. As the amount of solar radiation increases, the production values will also increase. This effect can be seen in Figure 30, where panel productions for three different scenarios are shown based on changes in solar radiation.

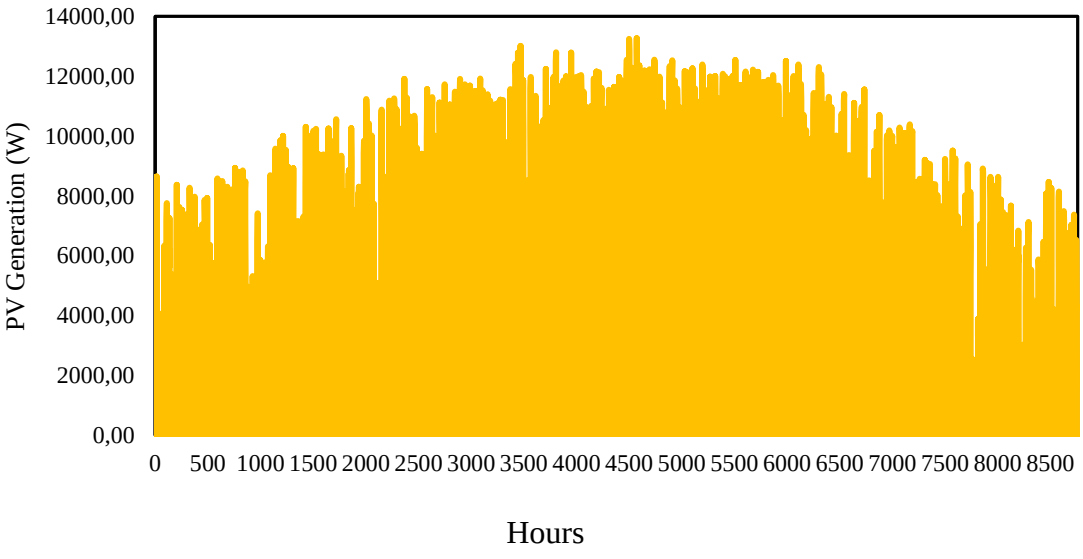

Figure 27. PV output power for the lowest radiation

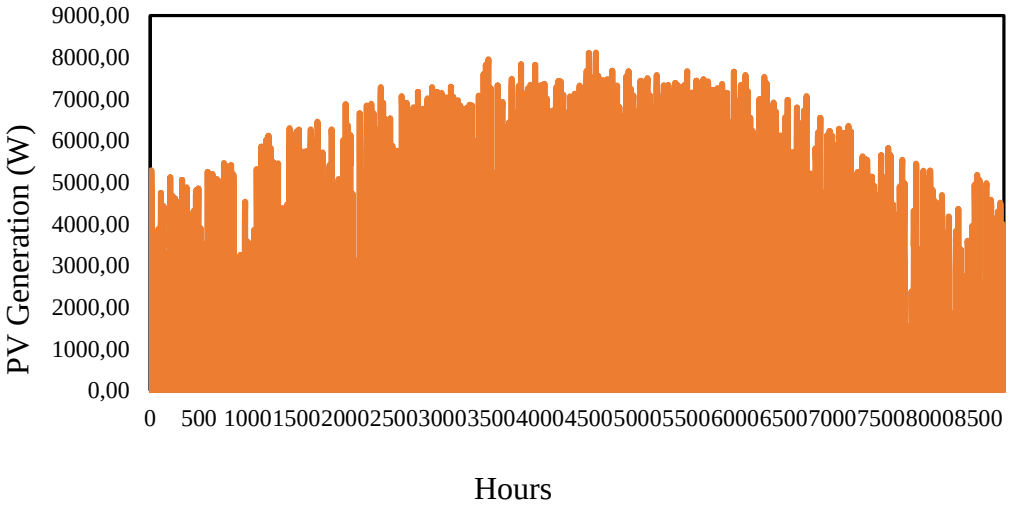

Figure 28. PV output power for the average radiation

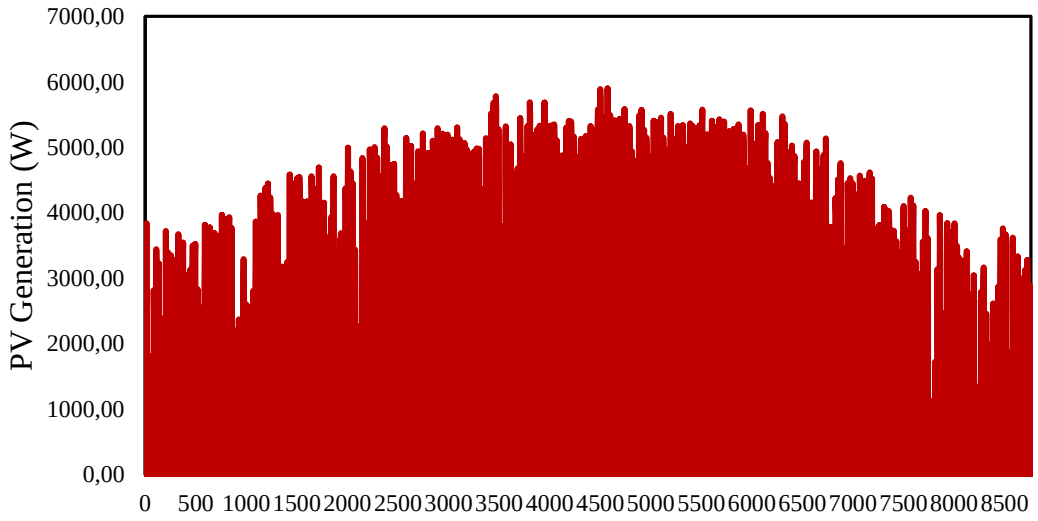

Figure 29. PV output power for the highest radiation

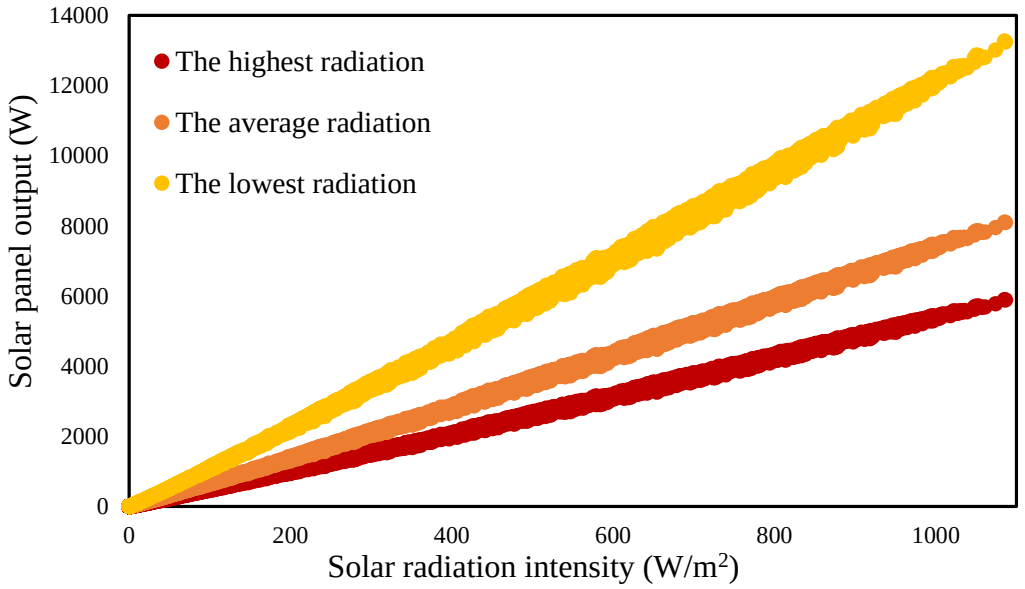

Figure 30. Solar panel output – solar radiation intensity

Figures 31-33 provide data on PV panel production values and grid support during times when the production falls short for three different radiation scenarios. It can be observed that PV production is utilized in two stations, namely the battery charging and the load. For the lowest radiation scenario, grid usage is zero between the months of March and October.

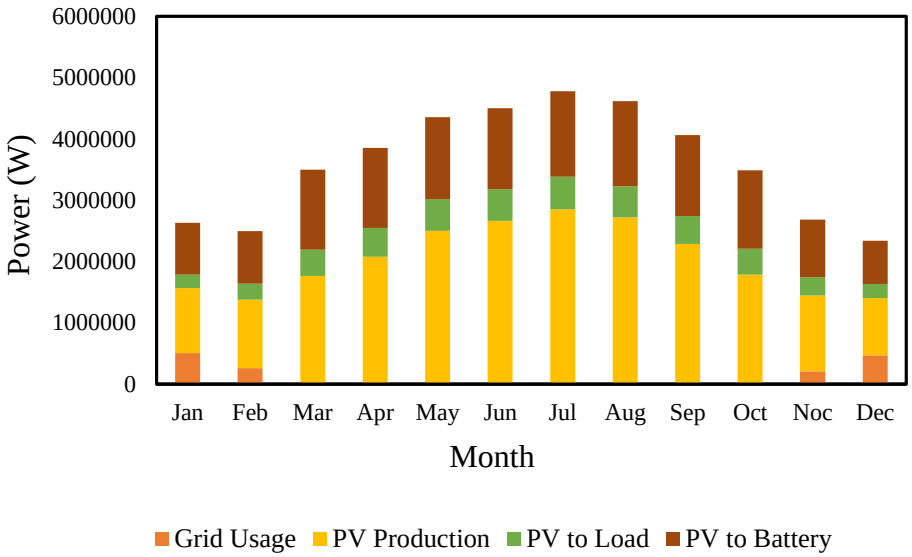

Figure 31. Grid usage-PV production for lowest radiation

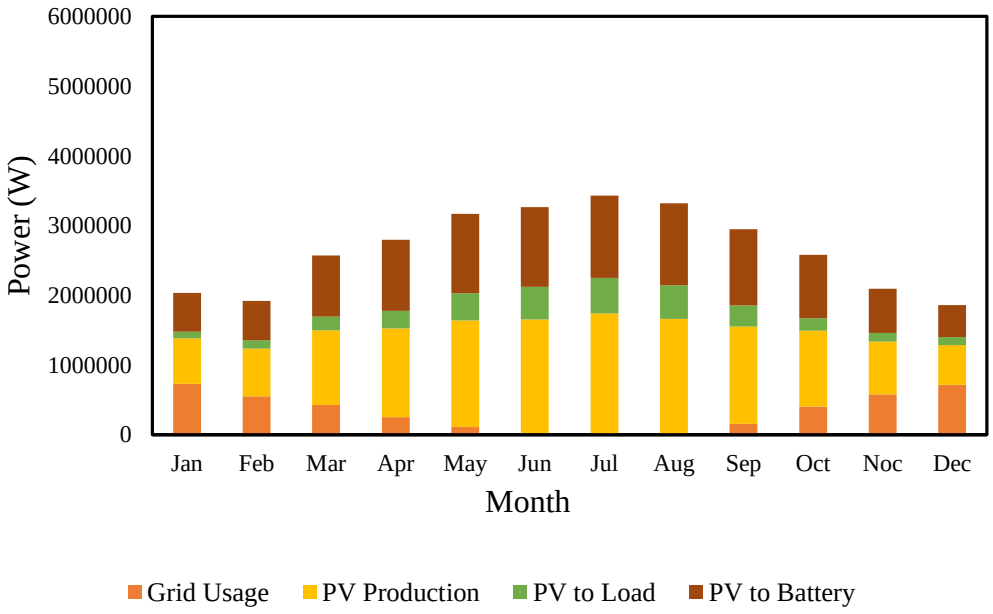

Figure 32. Grid usage-PV production for average radiation

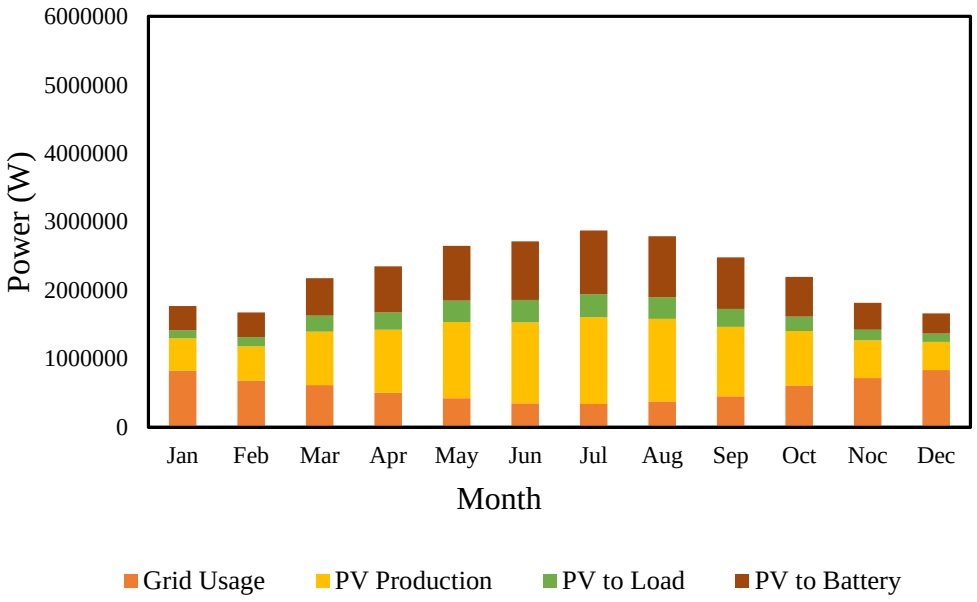

Figure 33. Grid usage-PV production for highest radiation

Figures 34-36 depict the relationship between monthly solar exergy variations, solar radiation changes, and ambient temperature. It is observed that July, August, and June exhibit the highest solar radiation and ambient temperature values across scenarios of lowest, highest, and average radiation levels. Similarly, these months demonstrate high solar energy values. The graphs indicate a direct relationship between global radiation, ambient temperature, and solar exergy, suggesting that higher radiation levels contribute to increased solar exergy generation.

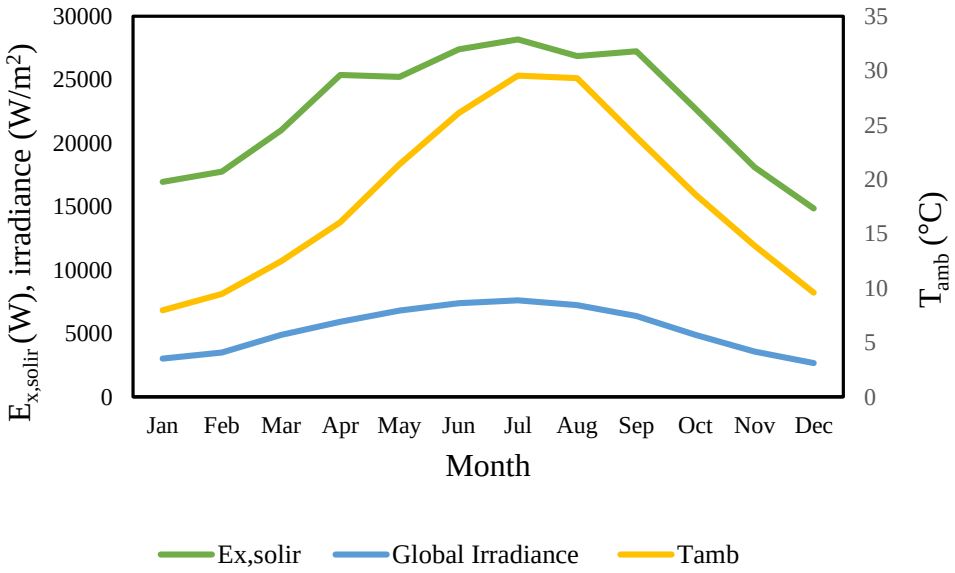

Figure 34. Solar exergy ($E_{x,solir}$), T_{amb} , global radiation for the lowest solar radiance

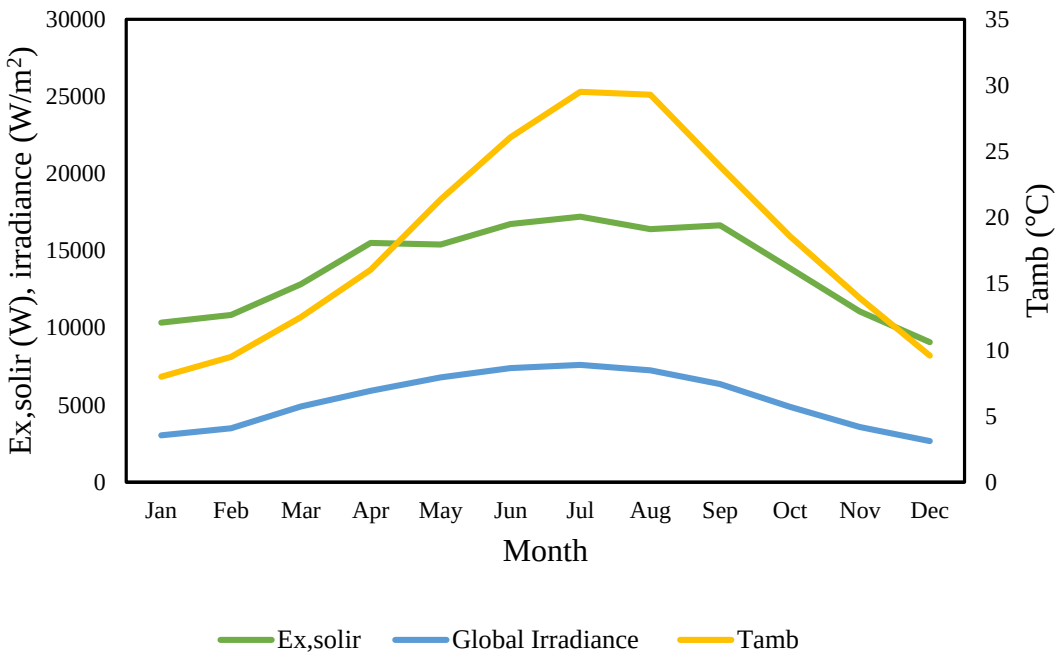

Figure 35. Solar exergy ($E_{x,solir}$), T_{amb} , global radiation for the average solar radiance

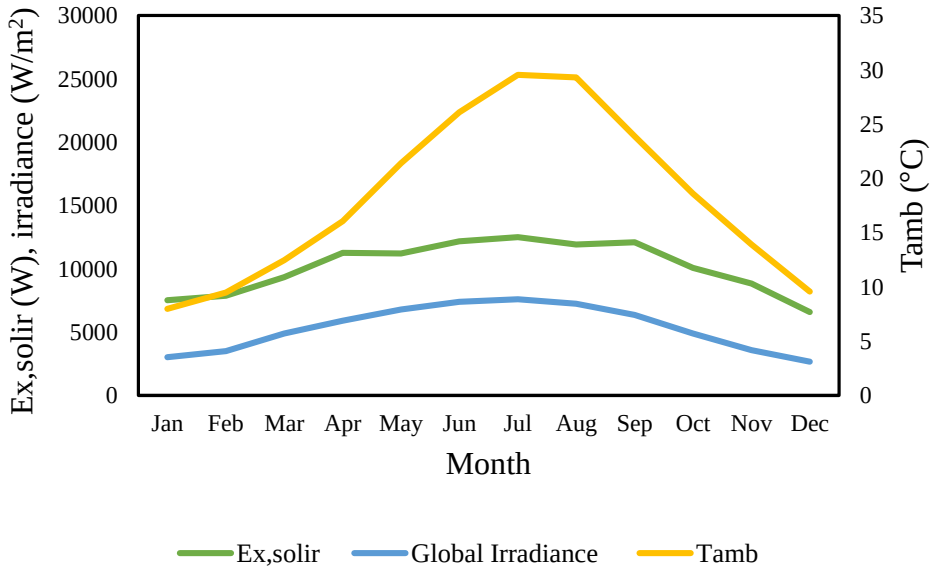

Figure 36. Solar exergy ($E_{x,solir}$), T_{amb} , global radiation for the highest solar radiance

Figures. 37-39. provide information on solar energy inputs, electrical exergy, thermal exergy, and output exergy values. As mentioned earlier, solar energy input is represented by solar exergy obtained in proportion to the incoming solar radiation. Based on the previous graphs, in the scenario considering low radiation, the solar exergy is approximately 15000 W during winter and 26000 W during summer. In the design considering the highest solar radiation values, the solar exergy is approximately 12000

W in summer and 7000 W in winter. In the design considering average radiation, these values are approximately 10000 W in winter and 16000 W in summer.

When examining the electrical output values obtained by multiplying the current and voltage values at the maximum power point, it is observed that the highest value is achieved in the design with low solar radiation, reaching 6000 W during summer and the lowest value of 3000 W during winter. In designs considering high and average solar radiation, the electrical outputs produced during summer are approximately 2600 W and 3600 W, respectively, while during winter, they are observed to be around 2000 W and 1500 W, respectively.

In terms of thermal outputs, an increase in thermal losses is observed due to a higher number of panels during winter. The higher number of panels indicates an increase in the panel area, leading to an increase in heat losses from the panel surfaces. Therefore, thermal losses in winter are higher compared to summer. When evaluating the thermal losses in winter based on the highest, average, and lowest radiation values, they are observed to be approximately 120 W, 160 W, and 260 W, respectively.

Looking at the graphs, it can be seen that the output exergy is lower than the input exergy. The output exergy is the sum of electrical energy and thermal energy. The reason why the electrical exergy, which represents the usable net energy, is lower than the solar exergy can be attributed to irreversible thermal losses.

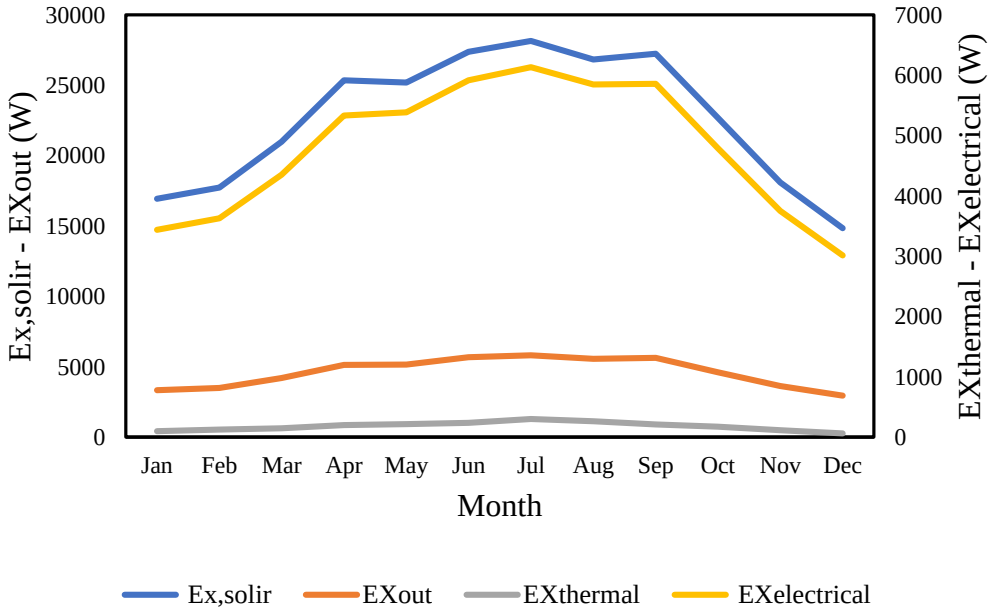

Figure 37. Input exergy ($E_{x,solir}$) -output exergy (EX_{out}) -thermal exergy ($EX_{thermal}$) and electrical exergy ($EX_{electrical}$) for the lowest radiation

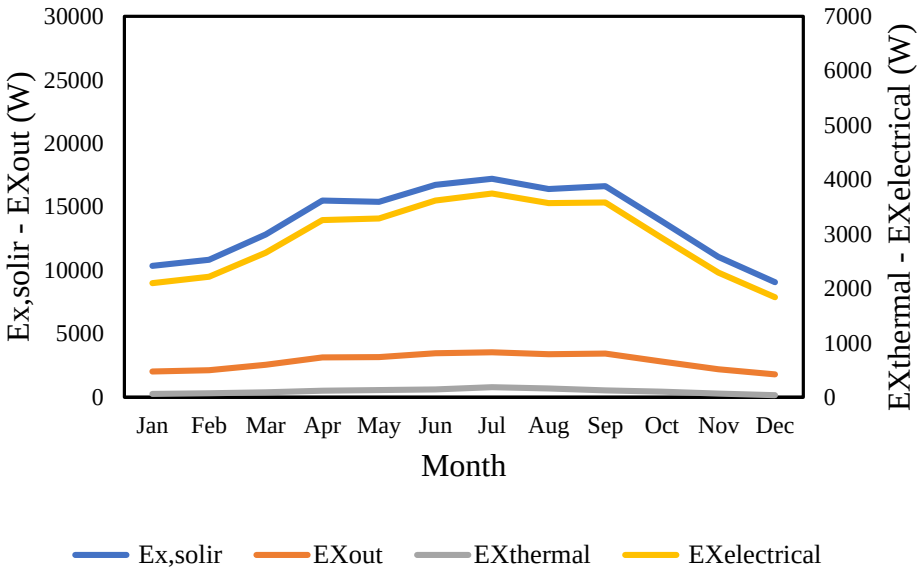

Figure 38. Input exergy ($E_{x,solir}$) -output exergy (EX_{out}) -thermal exergy ($EX_{thermal}$) and electrical exergy ($EX_{electrical}$) for the average radiation

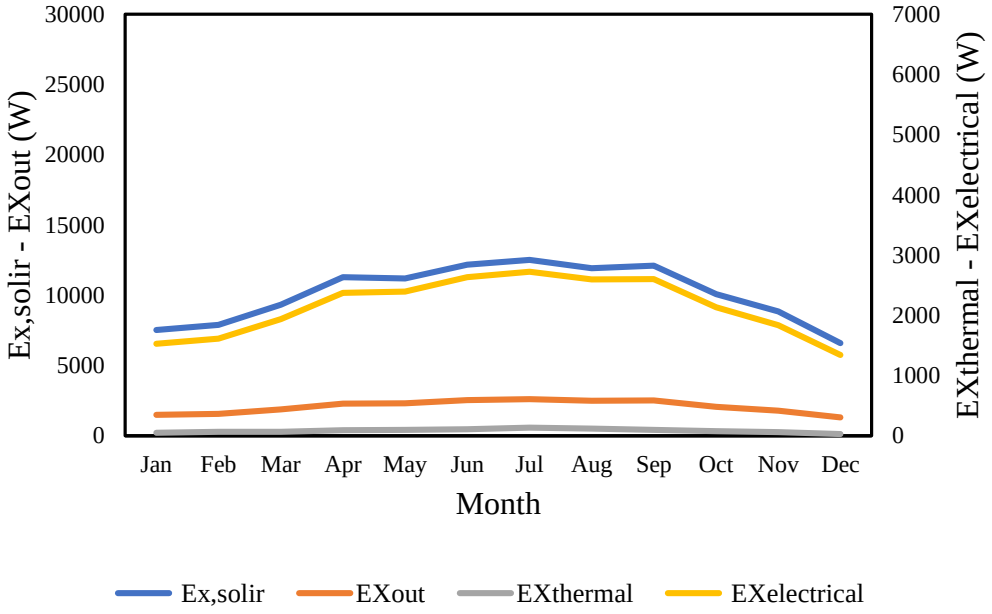

Figure 39. Input exergy ($E_{x,solir}$) -output exergy (EX_{out}) -thermal exergy ($EX_{thermal}$) and electrical exergy ($EX_{electrical}$) for the highest radiation

The variation of energy and exergy efficiencies by month is shown in Figure 40. The monthly changes in output exergy (the sum of thermal and electrical outputs) and solar exergy have contributed to the fluctuation of exergy efficiency, resulting in an increase or decrease on a monthly basis. Similarly, the changes in the ratio of production values in solar panels to solar radiation have led to differences in energy efficiencies across months. As can be seen, when we evaluate the energy and exergy efficiencies,

energy and exergy efficiencies off all scenarios are the same. This is because we use the same panels and the changing parameter is the panel areas. Although the energy generation values and output exergies differ for scenarios, when we examine the values as efficiency in the formula as a whole, the same values are obtained due to the proportional increase in the panel areas.

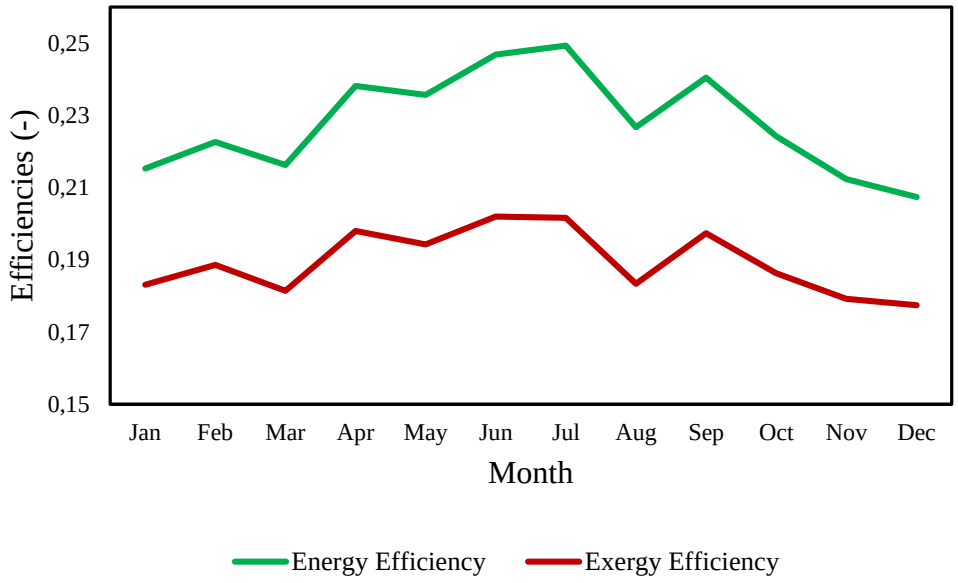

Figure 40. Energy and exergy efficiencies

4.3. Exergo-economic Analysis

Table 14 displays the panel, battery, inverter, and auxiliary equipment employed in the system designs, along with their associated costs, evaluated based on the lowest, average, and highest radiation levels.

Table 14. Equipment costs

Equipment	Unit Price ($)	Number of Units		
		The Lowest Radiation	The Average Radiation	The Highest Radiation
HTSAA solar 320W monocrystalline solar module (PCS)	135	36	22	16
GOODWE 5KW hybrid inverter 48V (PCS)	2800	1	1	1
RITAR 12V 200AH DG12-200 solar gel battery (PCS)	350	16	12	8
Solar construction ground mounting per module (SET)	65	36	22	16
Solar cable PV1-F black 1X6 mm^2 (mt)	1.5	60	60	60
Solar cable PV1-F red 1X6 mm^2 (mt)	1.5	60	60	60
Solar connector MC4 multicontact IP67 male (PCS)	2	2	2	2
Solar connector MC4 multicontact IP67 female (PCS)	2	2	2	2
PV and battery DC fuse panel (PCS)	125	1	1	1
Grid and load AC fuse panel (PCS)	115	1	1	1
Battery rack (per battery) (SET)	185	36	12	8
Assembly equipment (SET)	250	1	1	1
Transport and mounting services (PCS)	550	1	1	1
Engineering and project services (PCS)	400	1	1	1

When conducting a cost analysis for the system, annual maintenance and repair expenses should be determined, and the replacement periods of the equipment used should be identified for cost estimation. The annual maintenance and repair costs are assumed to be 5% of the initial investment cost. The battery replacement periods are set at 15 years for the lowest radiation scenario, 10 y for the average radiation scenario, and 9 years for the highest radiation scenario. The inverter replacement period is every 10 years.

The cost table for 20 years based on equipment replacement periods, maintenance operating expenses and initial investment costs is shown in Table 15.

Table 15. Capital and maintenance costs for 3 scenarios

	Cost ($)		
	The Lowest Radiation	**The Average Radiation**	**The Highest Radiation**
Initial investment	28,837.00	18,642.00	14,051.00
Operating maintenance	47,676.00	30,820.00	23,231.00
Battery replacement	11,088.00	17,129.00	10,555.00
Inverter replacement	11,419.00	11,419.00	11,419.00
Total	99,020.00	78,010.00	59,256.00

The R_{en} and R_{ex} are shown in Figures 41-43. for the lowest radiation, average radiation and highest radiation scenarios, respectively. The R value represents the ratio of energy and exergy losses to the system cost. During the summer months, there are losses in electricity production from solar panels due to temperature. As indicated in datasheets, solar panels have temperature coefficients. The temperature coefficient indicates how much efficiency of the solar panel will decrease when the temperature rises by 1°C. Therefore, losses increase during the summer months.

When considering the radiation scenarios, R values are higher in scenarios with the lowest radiation. Lower values are observed in scenarios with average radiation and the highest radiation levels. The reason for the difference is that during the winter period, a higher number of panels and components are used, leading both higher losses and investments. However, in scenarios with the average radiation and highest radiation, where the number of panels used is similar, the energy and exergy losses are close each other for these two scenarios.

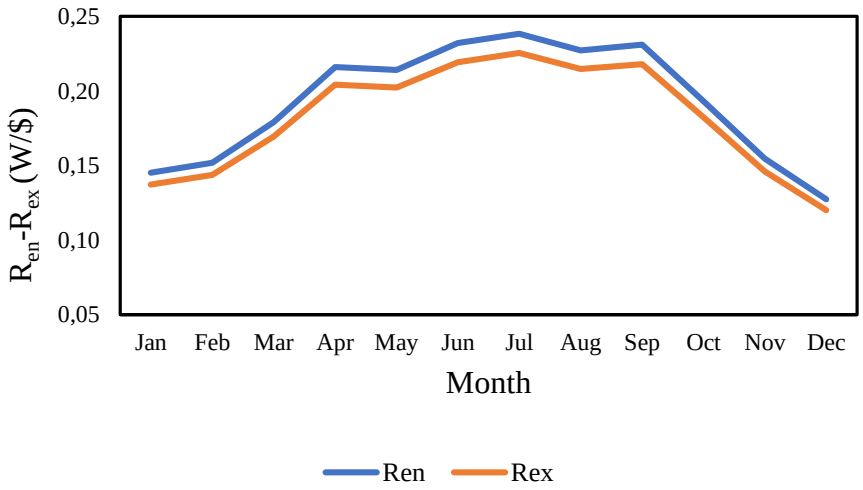

Figure 41. R_{en} and R_{ex} for the lowest radiation

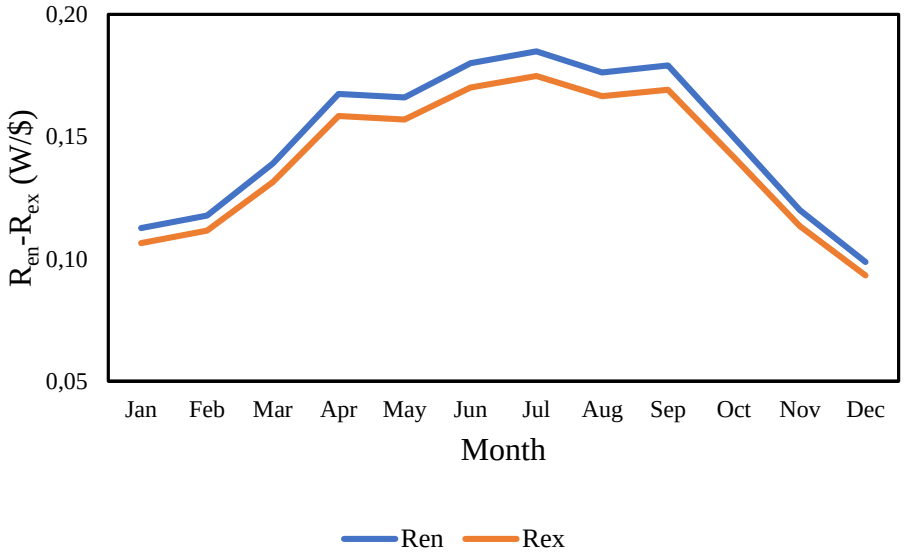

Figure 42. R_{en} and R_{ex} for the average radiation

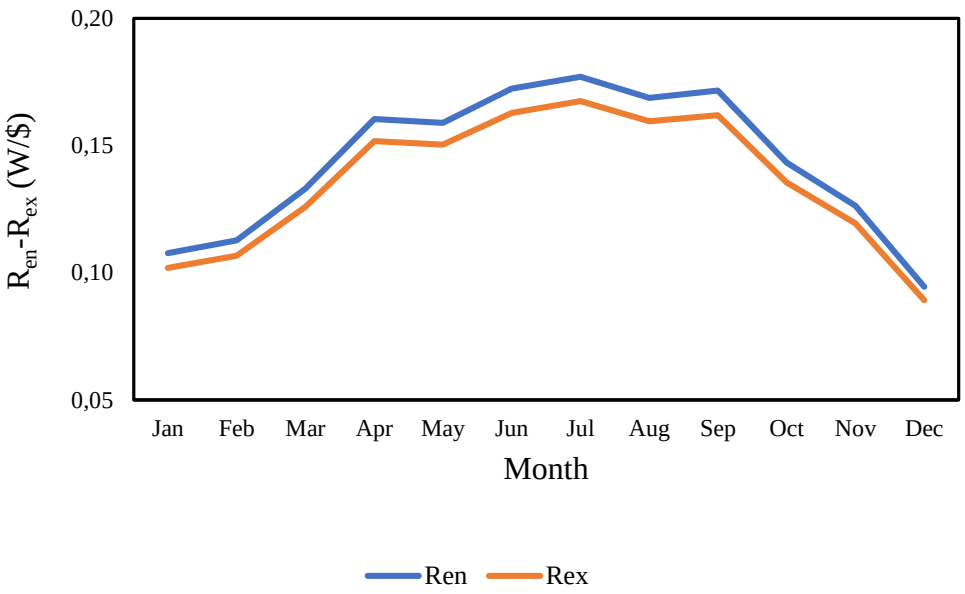

Figure 43. R_{en} and R_{ex} for the highest radiation

Other economic parameters such as net present value, payback period, cost of energy are given in Table 16.

Table 16. Economic parameters

	The Highest Radiation	**The Lowest Radiation**	**The Average Radiation**
NPV ($)	39,045.96	66,282.68	52,218.77
PP (year)	11,17	12,19	11.16
COE ($/kWh)	0.29	0.22	0.28

When evaluated based on economic parameters, considering the net present value, which represents the overall profit generated by the project over its lifetime, the scenario with the lowest radiation has the highest value at 66,282.68 $. However, when considering the payback period, the study conducted with the lowest radiation scenario has the longest duration at 12.19 y. Based on the above values, in the most optimal evaluation, the analysis conducted with the average radiation scenario, which has a net present value of 52,218.77 $ and a payback period of 11.16 y, may be a more sensible investment compared to the analysis conducted with the highest and lowest radiation scenarios. According to the cost of energy although the cost of energy is lower at 0.22 $/kWh compared to $0.28/kWh, when considering the payback periods and net present values,

the average radiation scenario will amortize itself in a shorter period and generate higher profits.

When payback periods are evaluated, long amortization periods such as 11 y or 12 y are observed. Factors such as supply shortages, high transportation costs for imported products, maintenance, labor costs for part replacements, and high inflation at the time of writing the thesis contribute to these extended payback periods. In addition to these costs, the integration of storage systems into renewable energy systems also leads to high expenses, which are significant parameters that extend the payback period.

CHAPTER 5

CONCLUSIONS

Currently, there is a global increase in demand for obtaining freshwater. Freshwater resources are gradually decreasing, leading to the adoption of seawater and brackish water desalination processes to meet freshwater needs. Water desalination is an energy-intensive process, and traditionally, this energy demand has been primarily met by fossil fuels. However, in recent times, there has been a shift towards using renewable energy sources, particularly solar and wind, to fulfill this energy demand.

This study focuses on a grid-connected geothermal desalination system with battery-supported PV system, aiming to increase its own energy self-consumption, namely minimizing grid dependency and maximizing the solar utilization. The system utilizes the used geothermal water from the Yenikale Geothermal Heat Center to produce freshwater through desalination. To meet the energy demand of the desalination system, PV-battery-grid-supported system designs were implemented. These designs were tailored for three different radiation values: the highest solar radiation, the lowest solar radiation, and the average solar radiation. Configurations with a 320 W PV panel and a 12 V 200Ah battery were used for the three different radiation values. The thermo-economic analysis of the system has been conducted, and considering exergy losses, a cost analysis has been performed using the economic analysis method. The TRNSYS software was utilized for modeling, and the results were analyzed for one year. The important outcomes extracted from the study are as follows.

When evaluating battery DOD (Depth of Discharge), as the DOD increases, the number of cycles the battery can go through during its lifespan will decrease. This will shorten the battery's overall usage life and may necessitate replacing the battery, leading to increased costs. As the battery DOD increases, the battery will be discharged to a deeper level. After deeper discharge, the battery will require more frequent recharging. During the recharging process, there will be more efficiency losses in the components.

From an energy analysis perspective, when comparing PV productions, the modeling conducted for the lowest radiation scenario (36 units of 320 W PV, 38400 Wh

battery) resulted in higher PV production compared to the average and highest radiation scenarios (which used 22 units of 320 W PV and 28800 Wh battery for the average radiation, and 18 units of 320 W PV and 19200 Wh battery for the highest radiation). This higher PV production is attributed to the larger number of PV units used in the lowest radiation scenario.

From an exergy analysis perspective, when examining the relationship between solar exergy and solar radiation, solar exergy refers to the usable solar energy that can be converted into electricity. The solar energy value increases as the amount of solar radiation increases. Solar radiation should be considered as an input value for solar exergy analysis, as it directly affects the amount of usable solar energy available for conversion into electricity.

When relating solar exergy and solar radiation to ambient temperature, we observe a direct relationship between these three parameters. In other words, during periods of high solar radiation, we also observe an increase in both solar exergy and ambient temperature.

We defined input exergy as the power obtained from PV modules related to radiation intensity. Output exergy includes both electrical and thermal energy. The highest electrical output was obtained in the lowest radiation scenario. When examining thermal exergy, again the highest value was observed in the lowest solar radiation scenario. We can explain this by the increased number of panels and, consequently, the increased panel area, leading to more heat loss from the panel surface.

When the exergo-economic analysis, which considers the energy and exergy loss rates, is examined in terms of $, the Ren and Rex values vary depending on the months. For summer months, the values are approximately 0.17 W/$, while for winter months, they are 0.11 W/$. Therefore, the average radiation scenario can be selected as the appropriate project method.

Considering the payback periods, the integration of storage systems into renewable energy systems causes high costs and the transportation costs of the materials used, maintenance, labor, part replacement costs extend the depreciation periods.

REFERENCES

Abdelkareem, Mohammad Ali, M El Haj Assad, Enas Taha Sayed, and Bassel Soudan. 2018. "Recent progress in the use of renewable energy sources to power water desalination plants." *Desalination* 435: 97-113.

Ahmad, GE, and J Schmid. 2002. "Feasibility study of brackish water desalination in the Egyptian deserts and rural regions using PV systems." *Energy Conversion and Management* 43 (18): 2641-2649.

Ajiwiguna, Tri Ayodha, Ga-Ram Lee, Byung-Ju Lim, Sung-Hoon Cho, and Chang-Dae Park. 2021. "Optimization of battery-less PV-RO system with seasonal water storage tank." *Desalination* 503: 114934. https://doi.org/https://doi.org/10.1016/j.desal.2021.114934. https://www.sciencedirect.com/science/article/pii/S0011916421000059.

Ajiwiguna, Tri Ayodha, Ga-Ram Lee, Byung-Ju Lim, Seok-Min Choi, and Chang-Dae Park. 2022. "Design strategy and economic analysis on various configurations of stand-alone PV-RO systems." *Desalination* 526: 115547.

Al-Karaghouli, Ali A, and LL Kazmerski. 2011. "Renewable energy opportunities in water desalination." *Desalination, trends and technologies*: 149-184.

Alatiqi, Imad, Hisham Ettouney, and Hisham El-Dessouky. 1999. "Process control in water desalination industry: an overview." *Desalination* 126 (1-3): 15-32.

Alkaisi, Ahmed, Ruth Mossad, and Ahmad Sharifian-Barforoush. 2017. "A review of the water desalination systems integrated with renewable energy." *Energy Procedia* 110: 268-274.

Alsheghri, Ammar, Saad Sharief, Shahid Rabbani, Nur Aitzhan, and Alejandro Galvan. 2015. *Design and Cost Analysis of a Reverse Osmosis Plant Integrated with Solar Photovoltaic for Masdar Institute*.

Atallah, Mohamed Osman, M. A. Farahat, Mohammed Elsayed Lotfy, and Tomonobu Senjyu. 2020. "Operation of conventional and unconventional energy sources to drive a reverse osmosis desalination plant in Sinai Peninsula, Egypt." *Renewable Energy* 145: 141-152. https://doi.org/https://doi.org/10.1016/j.renene.2019.05.138. https://www.sciencedirect.com/science/article/pii/S0960148119308110.

Barbier, Enrico. 2002. "Geothermal energy technology and current status: an overview." *Renewable and Sustainable Energy Reviews* 6 (1): 3-65. https://doi.org/https://doi.org/10.1016/S1364-0321(02)00002-3. https://www.sciencedirect.com/science/article/pii/S1364032102000023.

Bellos, Evangelos, Sasa Pavlovic, Velimir Stefanovic, Christos Tzivanidis, and Branka Nakomcic-Smaragdakis. 2019. "Parametric analysis and yearly performance of a trigeneration system driven by solar- dish collectors." *International Journal of Energy Research* 43. https://doi.org/10.1002/er.4380.

Bourouni, Karim, Tunis Tunisia, and Ariana Tunisia. 2005. "Application of Geothermal Energy for Brackish Water Desalination in the South of Tunisia."

Bundschuh, Jochen, Michał Kaczmarczyk, Noreddine Ghaffour, and Barbara Tomaszewska. 2021. "State-of-the-art of renewable energy sources used in water desalination: Present and future prospects." *Desalination* 508: 115035. https://doi.org/https://doi.org/10.1016/j.desal.2021.115035. https://www.sciencedirect.com/science/article/pii/S0011916421001065.

Chekir, Nihel. 2020. "Geothermal energy for sustainable water Desalination : case of Tunisia w & e international (water resources section)." *Water and Energy International* volume 63: 26-39.

Chu, Yinghao, and Peter Meisen. 2011. "Review and comparison of different solar energy technologies." *Global Energy Network Institute (GENI), San Diego, CA* 6: 1-56.

Cooley, Heather, Peter H Gleick, and Gary Hartman Wolff. 2006. Desalination, with a grain of salt: a California perspective. Pacific Institute for Studies in Development, Environment, and Security ….

Cunha, Diego PS, and Karen V Pontes. 2022. "Desalination plant integrated with solar thermal energy: A case study for the Brazilian semi-arid." *Journal of Cleaner Production* 331: 129943.

Duran Sahin, Ahmet, Ibrahim Dincer, and Marc A. Rosen. 2007. "Thermodynamic analysis of solar photovoltaic cell systems." *Solar Energy Materials and Solar Cells* 91 (2): 153-159. https://doi.org/https://doi.org/10.1016/j.solmat.2006.07.015. https://www.sciencedirect.com/science/article/pii/S0927024806003436.

Eke, Joyner, Ahmed Yusuf, Adewale Giwa, and Ahmed Sodiq. 2020. "The global status of desalination: An assessment of current desalination technologies, plants and capacity." *Desalination* 495: 114633.

Eltamaly, Ali, Emadadeen Ali, M. Boumaza, Sarwono Mulyono, and Muath Yasin. 2021. "Optimal Design of Hybrid Renewable Energy System for a Reverse Osmosis Desalination System in Arar, Saudi Arabia." *Arabian Journal for Science and Engineering* 46. https://doi.org/10.1007/s13369-021-05645-0.

Fairuz, Athaya, M. Faeshol Umam, M. Hasanuzzaman, N. A. Rahim, and I. M. Mujtaba. 2023. "Modeling and analysis of hybrid solar water desalination system for different scenarios in Indonesia." *Energy Conversion and Management* 276: 116475. https://doi.org/https://doi.org/10.1016/j.enconman.2022.116475. https://www.sciencedirect.com/science/article/pii/S0196890422012535.

Fanack Water. 2022. "Water Resources in Turkey." Accessed March 5, 2023. https://water.fanack.com/turkey/water-resources-in-turkey/.

Freire-Gormaly, M., and A. M. Bilton. 2019. "Design of photovoltaic powered reverse osmosis desalination systems considering membrane fouling caused by intermittent operation." *Renewable Energy* 135: 108-121. https://doi.org/https://doi.org/10.1016/j.renene.2018.11.065. https://www.sciencedirect.com/science/article/pii/S0960148118313843.

Fridleifsson, Ingvar, Ruggero Bertani, Ernst Huenges, John Lund, Árni Ragnarsson, and Ladislaus Rybach. 2008. "The possible role and contribution of geothermal energy to the mitigation of climate change." *IPCC Scoping Meeting on Renewable Energy Sources, Proceedings*: 59-80.

Ghafoor, A., T. Ahmed, A. Munir, Ch Arslan, and S. A. Ahmad. 2020. "Techno-economic feasibility of solar based desalination through reverse osmosis." *Desalination* 485: 114464. https://doi.org/https://doi.org/10.1016/j.desal.2020.114464. https://www.sciencedirect.com/science/article/pii/S0011916419316820.

Ghafoor, Abdul, and Anjum Munir. 2015. "Design and economics analysis of an off-grid PV system for household electrification." *Renewable and Sustainable Energy Reviews* 42: 496-502. https://doi.org/https://doi.org/10.1016/j.rser.2014.10.012. https://www.sciencedirect.com/science/article/pii/S1364032114008296.

Ghaithan, Ahmed M., Awsan Mohammed, and Laith Hadidi. 2022. "Assessment of integrating solar energy with reverse osmosis desalination." *Sustainable Energy Technologies and Assessments* 53: 102740.

https://doi.org/https://doi.org/10.1016/j.seta.2022.102740. https://www.sciencedirect.com/science/article/pii/S2213138822007883.
Ghanim, Dheya, Mohammed Fowzi, and Zaid Obaid. 2019. "Energy and Exergy Performance Calculation of Solar Photovoltaic/ Thermal Hybrid System under the Baghdad Environment." *Journal of University of Babylon for Engineering Sciences* 27: 130-141. https://doi.org/10.29196/jubes.v27i1.1976.
Gol. 2021. *Environment Report of Izmir-2021 (in Turkish).* https://webdosya.csb.gov.tr/db/ced/icerikler/izmir-ilcdr-2021-20220811104124.pdf.
Gomaa, Mohamed R., Ala'a K. Al-Bawwat, Mujahed Al-Dhaifallah, Hegazy Rezk, and Mohsen Ahmed. 2023. "Optimal design and economic analysis of a hybrid renewable energy system for powering and desalinating seawater." *Energy Reports* 9: 2473-2493. https://doi.org/https://doi.org/10.1016/j.egyr.2023.01.087. https://www.sciencedirect.com/science/article/pii/S2352484723000951.
Gökçek, Murat, and Öznur Begüm Gökçek. 2016. "Technical and economic evaluation of freshwater production from a wind-powered small-scale seawater reverse osmosis system (WP-SWRO)." *Desalination* 381: 47-57. https://doi.org/https://doi.org/10.1016/j.desal.2015.12.004. https://www.sciencedirect.com/science/article/pii/S0011916415301387.
Hakyemez, Can. 2019. *SU: Yeni Elmas.* https://www.tskb.com.tr/i/assets/document/pdf/TSKBBAkis_SUYeniElmas_Subat2019.pdf.
Helal, AM, SA Al-Malek, and ES Al-Katheeri. 2008. "Economic feasibility of alternative designs of a PV-RO desalination unit for remote areas in the United Arab Emirates." *Desalination* 221 (1-3): 1-16.
Hepbasli, Arif. 2008. "A key review on exergetic analysis and assessment of renewable energy resources for a sustainable future." *Renewable and Sustainable Energy Reviews* 12 (3): 593-661. https://doi.org/https://doi.org/10.1016/j.rser.2006.10.001. https://www.sciencedirect.com/science/article/pii/S1364032106001225.
HT-SAAE. 2020. "HT60-156M." https://www.ht-saae.com.au/pdf/ht/HT60-156M-en.pdf.
IEA. 2021. *Turkey 2021 Energy Policy Review.* (IEA). https://iea.blob.core.windows.net/assets/cc499a7b-b72a-466c-88de-d792a9daff44/Turkey_2021_Energy_Policy_Review.pdf.
IMM. 2023. *Annual District-Based Water Consumption Quantities (in Turkish).* https://acikveri.bizizmir.com/dataset/yillik-ilce-bazli-su-tuketim-miktarlari.
IRENA. 2012. *Water Desalination Using Renewable Energy.* https://www.irena.org/publications/2012/Mar/Water-Desalination-Using-Renewable-Energy.
Karavas, Christos-Spyridon, Konstantinos G Arvanitis, George Kyriakarakos, Dimitrios D Piromalis, and George Papadakis. 2018. "A novel autonomous PV powered desalination system based on a DC microgrid concept incorporating short-term energy storage." *Solar Energy* 159: 947-961.
Karellas, Sotirios, Konstantinos Terzis, and Dimitrios Manolakos. 2011. "Investigation of an autonomous hybrid solar thermal ORC–PV RO desalination system. The Chalki island case." *Renewable Energy* 36 (2): 583-590.
Khan, Meer AM, Shafiqur Rehman, and Fahad A Al-Sulaiman. 2018. "A hybrid renewable energy system as a potential energy source for water desalination using

reverse osmosis: A review." *Renewable and Sustainable Energy Reviews* 97: 456-477.

Koschikowski, Joachim, Marcel Wieghaus, and Matthias Rommel. 2003. "Solar thermal-driven desalination plants based on membrane distillation." *Desalination* 156 (1-3): 295-304.

Kumar, Siddhant, Manish Kumar, Sumanta Chowdhury, Bharat Singh Rajpurohit, and Jaspreet Kaur Randhawa. 2022. "Environmental concerns and long-term solutions for solar-powered water desalination." *Journal of Cleaner Production*: 131180.

Luis, Patricia, and Bart Van der Bruggen. 2014. "Exergy analysis of energy-intensive production processes: advancing towards a sustainable chemical industry." *Journal of Chemical Technology & Biotechnology* 89 (9): 1288-1303. https://doi.org/https://doi.org/10.1002/jctb.4422. https://doi.org/10.1002/jctb.4422.

Ma, Qingfen, and Hui Lu. 2011. "Wind energy technologies integrated with desalination systems: Review and state-of-the-art." *Desalination* 277 (1-3): 274-280.

Mahmoud, Marwan M. 2003. "Solar electric powered reverse osmosis water desalination system for the rural village, Al Maleh: design and simulation." *International Journal of Sustainable Energy* 23 (1-2): 51-62.

Mahmoud, Marwan M., and Imad H. Ibrik. 2006. "Techno-economic feasibility of energy supply of remote villages in Palestine by PV-systems, diesel generators and electric grid." *Renewable and Sustainable Energy Reviews* 10 (2): 128-138. https://doi.org/https://doi.org/10.1016/j.rser.2004.09.001. https://www.sciencedirect.com/science/article/pii/S1364032104001224.

Malviya, Rajkumar, Ayush Agrawal, and Prashant V Baredar. 2021. "A comprehensive review of different heat transfer working fluids for solar thermal parabolic trough concentrator." *Materials Today: Proceedings* 46: 5490-5500.

Map TR. 2023. "Izmir Map (in Turkish)." Accessed March 8, 2023. https://www.haritatr.com/harita/Izmir/92307.

MENR. 2022. "Sun (in Turkish)." Accessed March 5,2023. https://enerji.gov.tr/eigm-yenilenebilir-enerji-kaynaklar-gunes#:~:text=%C3%9Clkemiz%2C%20co%C4%9Frafi%20konumu%20nedeniyle%20%C3%B6nemli,kWh%2Fm2%20olarak%20hesaplanm%C4%B1%C5%9Ft%C4%B1r.

Mostafaeipour, Ali, Mojtaba Qolipour, Mostafa Rezaei, and Erfan Babaee-Tirkolaee. 2019. "Investigation of off-grid photovoltaic systems for a reverse osmosis desalination system: A case study." *Desalination* 454: 91-103. https://doi.org/https://doi.org/10.1016/j.desal.2018.03.007. https://www.sciencedirect.com/science/article/pii/S0011916417318362.

Padmavathi, K., and S. Arul Daniel. 2013. "Performance analysis of a 3MWp grid connected solar photovoltaic power plant in India." *Energy for Sustainable Development* 17 (6): 615-625. https://doi.org/https://doi.org/10.1016/j.esd.2013.09.002. https://www.sciencedirect.com/science/article/pii/S0973082613000744.

Petela, Richard. 2008. "An approach to the exergy analysis of photosynthesis." *Solar Energy* 82 (4): 311-328. https://doi.org/https://doi.org/10.1016/j.solener.2007.09.002. https://www.sciencedirect.com/science/article/pii/S0038092X07001983.

Pietrasanta, Ariana M., Sergio F. Mussati, Pio A. Aguirre, Tatiana Morosuk, and Miguel C. Mussati. 2022. "Water-renewable energy Nexus: Optimization of geothermal energy-powered seawater desalination systems." *Renewable Energy* 196: 234-

246. https://doi.org/https://doi.org/10.1016/j.renene.2022.06.146. https://www.sciencedirect.com/science/article/pii/S0960148122009867.
Pouyfaucon, Arturo Buenaventura, and Lourdes García-Rodríguez. 2018. "Solar thermal-powered desalination: A viable solution for a potential market." *Desalination* 435: 60-69.
Racquel Lovelace. 2015. "Measured and Predicted Performance of a

Photovoltaic Grid-Connected System in a Humid

Subtropical Climate." MSc. Thesis, Mechanical Engineering Department, University of Texas at Tyler.
Rahimi, Bijan, Hamed Shirvani, Ali Asghar Alamolhoda, Fathollah Farhadi, and Mohammadreza Karimi. 2021. "A feasibility study of solar-powered reverse osmosis processes." *Desalination* 500: 114885.
Rawat, Rahul, Ravita Lamba, and S. C. Kaushik. 2017. "Thermodynamic study of solar photovoltaic energy conversion: An overview." *Renewable and Sustainable Energy Reviews* 71: 630-638. https://doi.org/https://doi.org/10.1016/j.rser.2016.12.089. https://www.sciencedirect.com/science/article/pii/S1364032116311455.
Razi, Faran, Ibrahim Dincer, and Kamiel Gabriel. 2020. "Exergoeconomic analysis of a new integrated copper-chlorine cycle for hydrogen production." *International Journal of Hydrogen Energy* 45 (55): 30042-30055. https://doi.org/https://doi.org/10.1016/j.ijhydene.2020.08.271. https://www.sciencedirect.com/science/article/pii/S0360319920333309.
Reddy, KV, and N Ghaffour. 2007. "Overview of the cost of desalinated water and costing methodologies." *Desalination* 205 (1-3): 340-353.
Ritar Power. 2020. "RITAR-DG12-200 (12V200Ah)." https://www.ritarpower.com/?gclid=Cj0KCQjwz8emBhDrARIsANNJjS41XF9eC9u3kHUSciDCm7q-VJF99Iw5ROToQtdOBNggibKQKgEMjzcaAjMXEALw_wcB.
Rosales-Asensio, Enrique, David Borge-Diez, Ana Pérez-Hoyos, and Antonio Colmenar-Santos. 2019. "Reduction of water cost for an existing wind-energy-based desalination scheme: A preliminary configuration." *Energy* 167: 548-560. https://doi.org/https://doi.org/10.1016/j.energy.2018.11.004. https://www.sciencedirect.com/science/article/pii/S0360544218322084.
Sarathe, Sakshi, Prashant V Baredar, Gaurav Dwivedi, Sagar Tapdiya, and Adarsh Gaurav. 2022. "Review of various types of renewable-powered desalination technologies with economic analysis." *Materials Today: Proceedings* 56: 326-335.
Sarhaddi, Faramarz, Said Farahat, Hossein Ajam, and A. Behzadmehr. 2009. "Exergetic Optimization of a Solar Photovoltaic Array." *Journal of Thermodynamics* 2009. https://doi.org/10.1155/2009/313561.
Srivastava, Tulika. 2013. "Energy and exergy analysis of 36 W solar photovoltaic module." *International Journal of Ambient Energy*. https://doi.org/10.1080/01430750.2013.770799.
Stefano, Farne, Giovenzana Valentina, Beghi Roberto, Lavanga Vito, and Guidetti Riccardo. 2021. "Setting up of a cost-effective continuous desalination plant based on coupling solar and geothermal energy." *Desalination* 500: 114854.
Talebizadehsardari, P., M. A. Ehyaei, A. Ahmadi, D. H. Jamali, R. Shirmohammadi, A. Eyvazian, A. Ghasemi, and Marc A. Rosen. 2020. "Energy, exergy, economic, exergoeconomic, and exergoenvironmental (5E) analyses of a triple cycle with

carbon capture." *Journal of CO2 Utilization* 41: 101258. https://doi.org/https://doi.org/10.1016/j.jcou.2020.101258. https://www.sciencedirect.com/science/article/pii/S2212982020305679.

TEIAS. 2023a. "Installed Capacity Reports (in Turkish)." Accessed March 27,2023. https://www.teias.gov.tr/kurulu-guc-raporlari.

---. 2023b. "Türkiye Electricity Statistics (in Turkish)." Accessed March 3, 2023. https://ytbsbilgi.teias.gov.tr/ytbsbilgi/frm_istatistikler.jsf.

Tomaszewska, Barbara, Gulden Gokcen Akkurt, Michał Kaczmarczyk, Wiesław Bujakowski, Nazli Keles, Yakubu A. Jarma, Alper Baba, Marek Bryjak, and Nalan Kabay. 2021. "Utilization of renewable energy sources in desalination of geothermal water for agriculture." *Desalination* 513. https://doi.org/10.1016/j.desal.2021.115151.

TUBITAK-NCBR. 2022. "Water-Energy-Food Nexus: Geothermal water for agriculture (Project No: 118Y490)." http://www.geo4food.com/Water-Energy-Food

Tzivanidis, Christos, Evangelos Bellos, and Kimon Antonopoulos. 2016. "Energetic and financial investigation of a stand-alone solar-thermal Organic Rankine Cycle power plant." *Energy Conversion and Management* 126: 421-433. https://doi.org/10.1016/j.enconman.2016.08.033.

Uyduranoğlu Öktem, Ayşe and Ayça Aksoy. 2015. *Turkey's Water Risks Report (in Turkish).* http://awsassets.wwftr.panda.org/downloads/turkiyenin_su_riskleri__raporu_web.pdf.

Vidyanandan, KV. 2017. "An overview of factors affecting the performance of solar PV systems." *Energy Scan* 27 (28): 216.

Voutchkov, Nikolay. 2018. "Energy use for membrane seawater desalination–current status and trends." *Desalination* 431: 2-14.

WRI. 2015. "Water Stress by Country: 2040." Accessed March 3, 2023. https://reliefweb.int/map/world/water-stress-country-2040.

Wright, Natasha C. 2014. "Justification for community-scale photovoltaic-powered electrodialysis desalination systems for inland rural villages in India." *Desalination* 352: 82-91.

Yazdanpanahi, Javad, Faramarz Sarhaddi, and Mohsen Mahdavi Adeli. 2015. "Experimental investigation of exergy efficiency of a solar photovoltaic thermal (PVT) water collector based on exergy losses." *Solar Energy* 118: 197-208. https://doi.org/https://doi.org/10.1016/j.solener.2015.04.038. https://www.sciencedirect.com/science/article/pii/S0038092X15002443.

Zachary, Justin, and Colleen M Layman. 2010. "Adding Desalination to Solar Hybrid and Fossil Plants." *Power* 154 (5): 104-104.

Zhang, Yue, AN Anoopkumar, Embalil Mathachan Aneesh, Arivalagan Pugazhendhi, Parameswaran Binod, Mohammed Kuddus, Ashok Pandey, Mukesh Kumar Awasthi, and Raveendran Sindhu. 2023. "Advancements in the energy-efficient brine mining technologies as a new frontier for renewable energy." *Fuel* 335: 127072.